

## **About Rigaku**



### Who We Are

Since its inception in 1951, Rigaku has been at the forefront of analytical and industrial instrumentation technology. Today, with hundreds of major innovations to their credit, the Rigaku group of companies are world leaders in the fields of general X-ray diffraction, thin film analysis, X-ray fluorescence spectrometry, small angle X-ray scattering, protein and small molecule

X-ray crystallography, Raman spectroscopy, X-ray optics, semiconductor metrology, X-ray sources, computed tomography, nondestructive testing and thermal analysis.

### **Corporate Mission**

To contribute to the enhancement of humanity through scientific and technological development.

### Products mentioned in this book



#### SmartLab SE

Highly versatile multipurpose X-ray diffractometer with built-in intelligent guidance.



#### MiniFlex XpC

Compact X-ray diffractometer for quality control of materials that is easy to use and is ideal for routine work.



#### **MiniFlex**

New 6th-generation general purpose benchtop XRD system for phase i.d and phase quantification.



#### SmartLab

Advanced state-of-the-art highresolution XRD system powered by Guidance expert system software.



#### Supermini200

Benchtop tube below sequential WDXRF spectrometer analyzes O through U in solids, liquids and powders.



#### **ZSX Primus IV**

High power, tube above, sequential WDXRF spectrometer with new ZSX Guidance expert system software.



#### **XES Chimica**

XES Chimica is a chemical state analyzer utilizing a double crystal spectrometer for precise X-ray emission spectroscopy. Sample introduction chamber is available as option.



#### XtaLAB Synergy-ED

A fully integrated electron diffractometer for measuring submicron crystals, utilizing a seamless workflow from data collection to structure determination of crystal structures.



#### nano3DX

True submicron resolution CT scanner with the parallel beam geometry combined with an ultrabright 1200 W rotating anode X-ray source for best image quality.

### Products mentioned in this book



#### CT Lab HV

High-resolution and high-voltage industrial X-ray CT scanner with unrivaled application support.



#### CT Lab HX

Flexible and versatile benchtop micro-CT scanner.



#### **NANOPIX Mini**

Small and wide angle X-ray scattering instrument designed for nano-structure analyses.



#### DSCvesta2

Differential scanning calorimeter with high sensitivity, high performance and low noise, realized by a compact furnace.



### NEX DE / NEX DE VS

60 kV EDXRF for rapid analysis. VS model offers variable small spot analysis with an integrated camera for precise sample positioning.



#### TMA8311

Thermomechanical analyzer with high-sensitivity, high-precision measurement by the differential method.



#### STA/HUM-1

High-concentration humidity controlled STA.

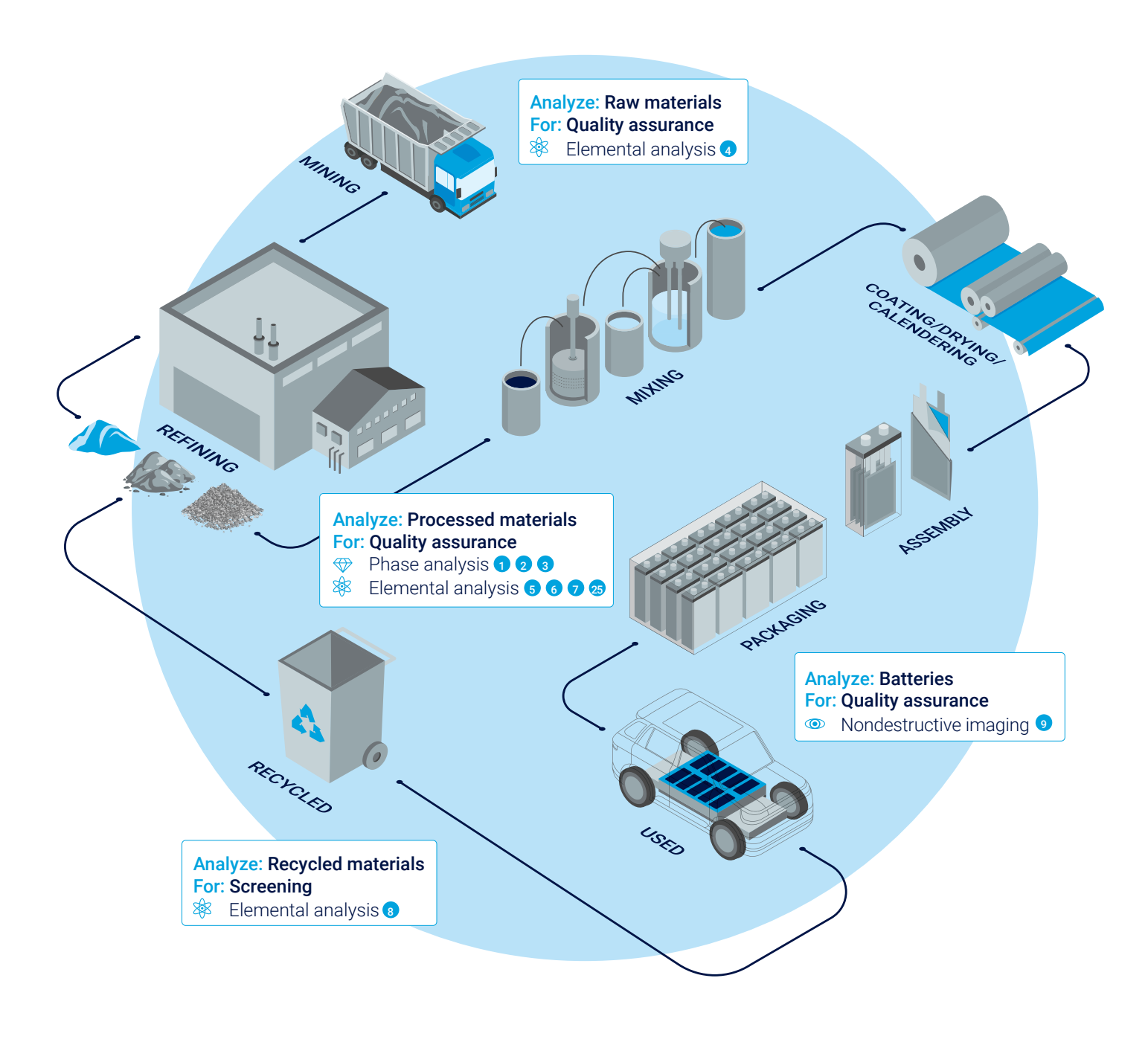


#### TMA/HUM-1

High-concentration humidity controlled TMA.

### Lithium Ion Battery Workflow

Rigaku's analysis technologies support safer and more efficient battery production.



<sup>#</sup> Application example ID (See Battery application book)

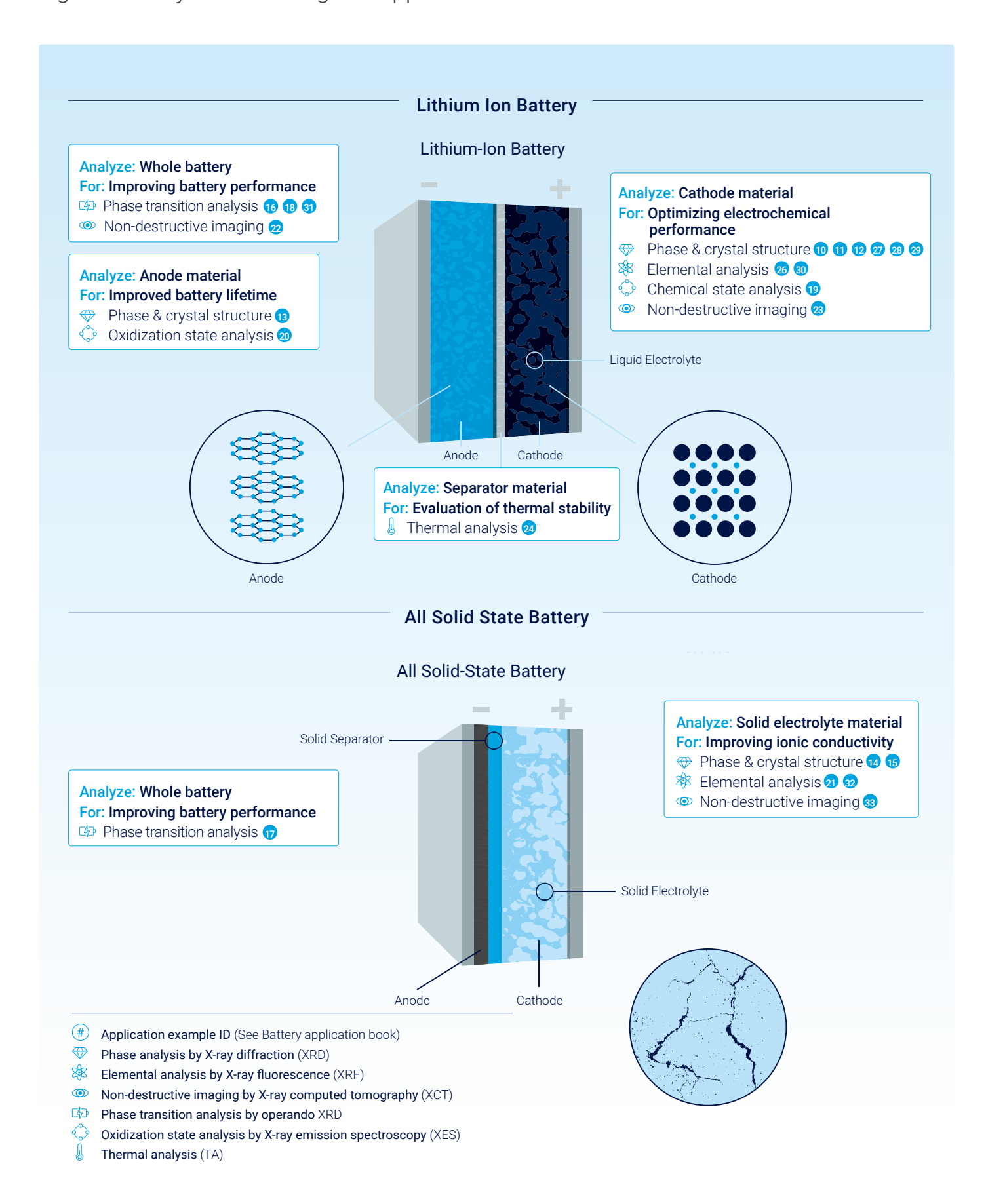
The Phase analysis by X-ray diffraction (XRD)

Elemental analysis by X-ray fluorescence (XRF)

Non-destructive imaging by X-ray computed tomography (XCT)

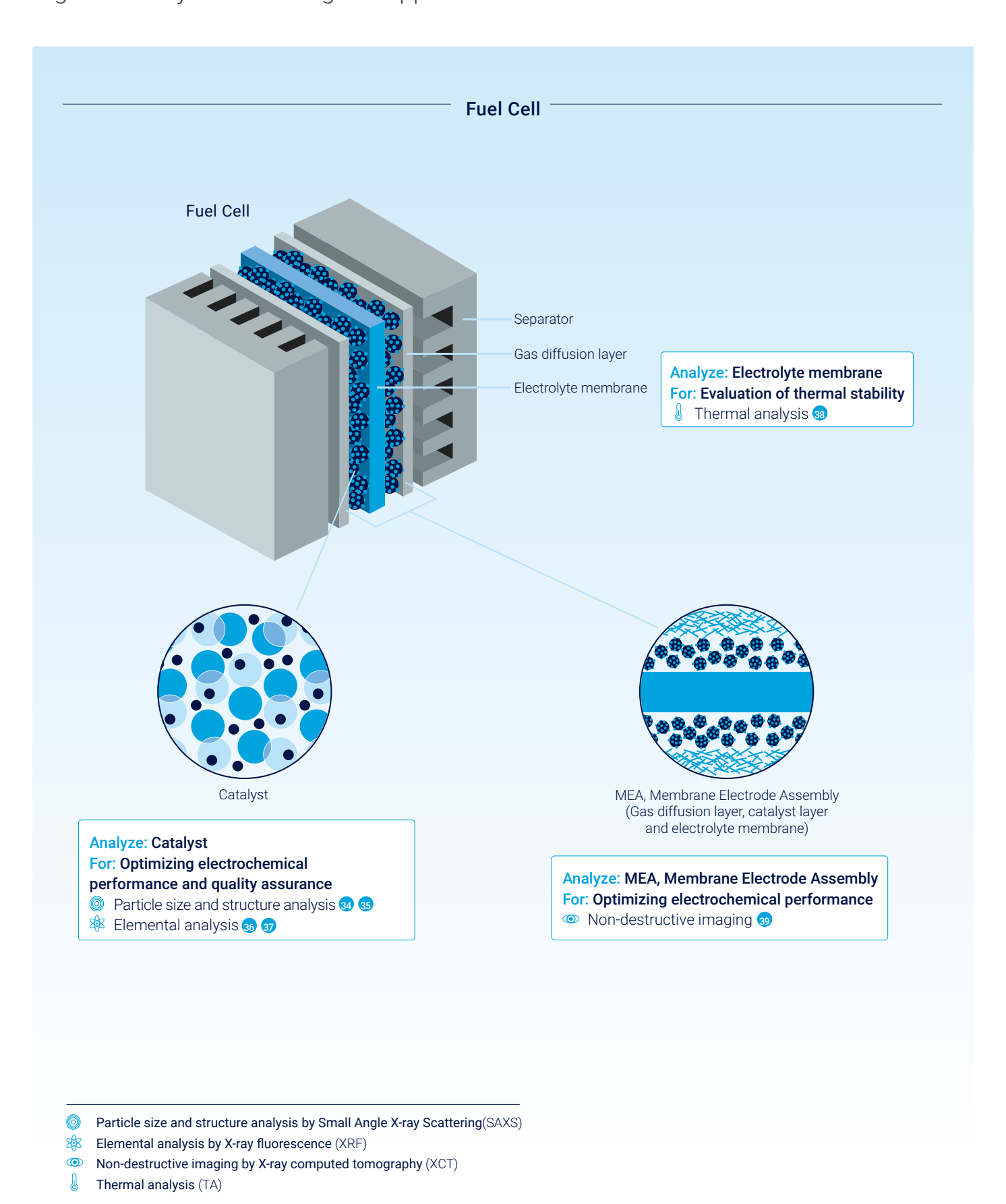
### Lithium Ion or Sodium Ion Battery Research & Development

Rigaku's analysis technologies support R&D for safer and more efficient batteries.



### **Fuel Cell**

Rigaku's analysis technologies support R&D for safer and more efficient cells.





# Qualitative Analysis of Impurities (Sulfate) in Mixed Nickel-Cobalt Sulfide

Analysis: materials

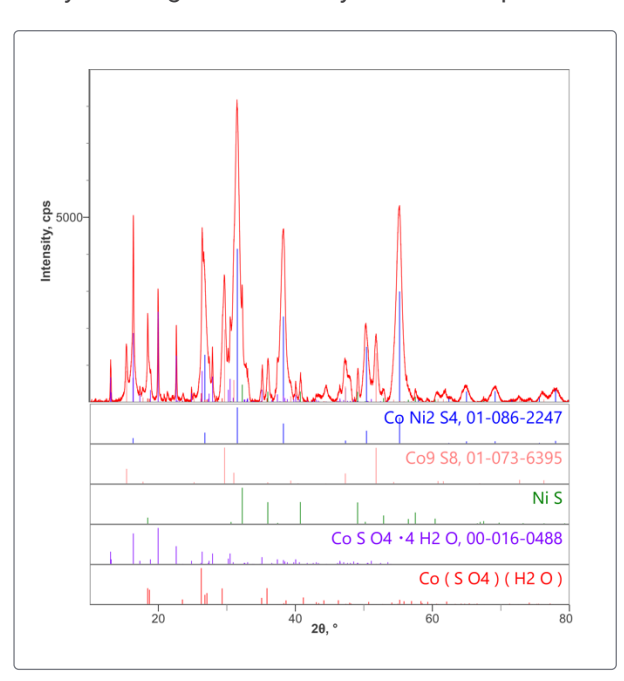
Processed

**Analyzed materials:**Mixed nickel-cobalt sulfide

Use:

Quality assurance

To ensure the quality of mixed nickel-cobalt sulfide, a raw material used to make batteries, the sulfate content needs to be minimized. Using XRD makes it possible to distinguish between sulfide and sulfate. Performing quantitative analysis using Rietveld analysis makes it possible to detect component amounts as well.



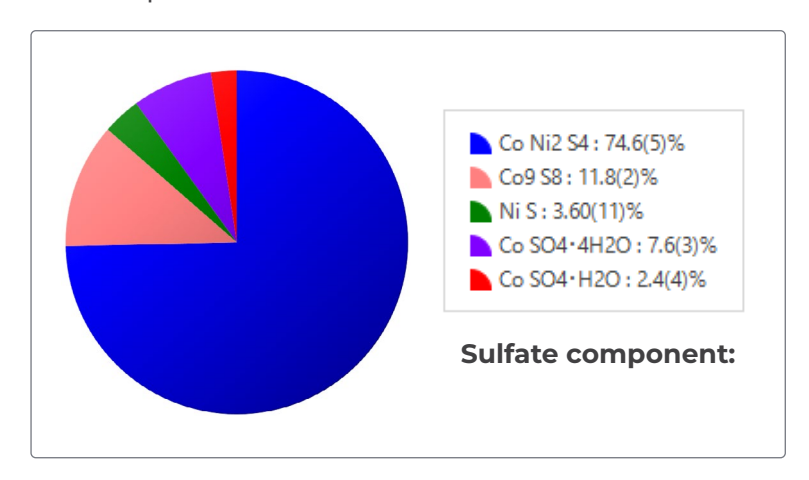
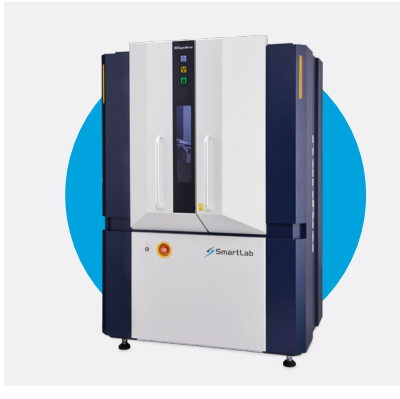


Figure 2: Results of quantitative analysis using Rietveld analysis

(Sulfate component has a 10% residual)

**Figure 1:** Qualitative analysis (5 components identified)

**Conclusion:** As a result of this analysis, a 10% residual was detected for the sulfate component. With the acceptable amount of sulfate component set to 1% or lower, it can be easily determined based on the result that this batch contains an anomaly.



**Equipment Used:** SmartLab SE

**Analysis Method:**Qualitative/quantitative analysis





### **Lattice Constant and Crystallite Diameter** Management for NCM Cathode Material

**Analysis:** materials

Processed

**Analyzed materials:** Li(Ni, Co, Mn, )O, NCM

Use: Quality assurance

With cathode material NCM, the lattice constant changes according to the composition, and electrical performance changes according to crystallite diameter. Because of these factors, lattice constant and crystallite diameter management is required to optimize this material. Using the EasyX plug-in for SmartLab Studio II software makes it possible to perform everything from measurement to results management with simple operations.



EasyX CSV Analysis Result M Peak Analysis Creat... a, and Sample Name size, ang. LiNi0.6Co0.2Mn0.2O2 2.870371 14.22 1609 LiNi0.5Co0.2Mn0.3O2 2.870467 14.243998 3018.85810 O) 14.244134 2.871882 4367.86698 LiNi0.5Co0.2Mn0.3O2 10:22:... 2.873919 LiNi0.5Co0.2Mn0.3O2 2.872651 14.248155 3352.29789 LiNi0.5Co0.2Mn0.3O2 14.243266 2.863349 1822.12753 LiNi1/3Co1/3Mn1/3... LiNi0.82Co0.15Mn0.... 2.869841 1260.40630

Figure 1: EasyX measurement screen (Executed in three steps:

Figure 2: EasyX results display screen

(1) Select measurement sample

(2) Select measurement analysis conditions

(3) Press the Start button)

(Arbitrary items such as the lattice constant and crystallite diameter can be designated)

Conclusion: EasyX can be operated with ease even by people who lack familiarity with XRD. Measurement, analysis and results display can be managed and analyzed through the software.



**Equipment Used:** MiniFlex XpC

**Analysis Method:** Rietveld analysis



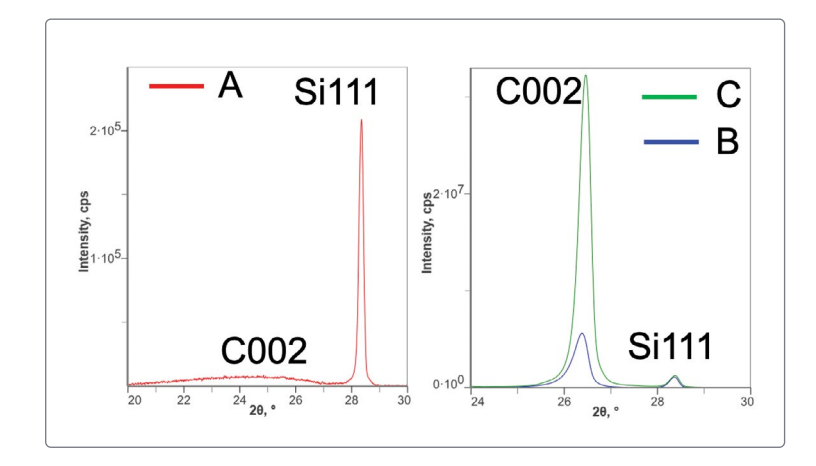


# Management of Graphitization Degree for Graphite Anode Material

Analysis: Processed Analyzed materials: C (Graphite)

**Use:** Quality assurance

The crystallinity of anode material graphite is known to be related to battery capacity. Through analysis of d-spacing, crystallite diameter L and graphitization degree  $P_1$  ( $d_{002}$ =3.354P1+3.44(1-P1)), it is possible to quantitatively evaluate and manage that crystallinity. Additionally, in Japan, measurement methods are standardized according to JIS R7651:2024, which uses Si as an internal standard.



Sample	d <sub>002</sub> (Å)	L <sub>002</sub> (Å)	P <sub>1</sub>
А	3.44	14	0
В	3.371	575	0.76
С	3.363	1587	0.85

Figure 1: XRD profile for graphite samples A, B and C

**Table 1:** Results of calculating  $d_{002}$ ,  $L_{002}$  and graphitization degree for Graphite Samples A, B and C (Graphitization progresses in the order of A, B and C)

**Conclusion:** To ensure the quality of graphite, it is necessary to manage parameters related to the degree of graphitization. With sample A, because there is no progression in the graphitization degree, that sample would be deemed unsuitable as a anode material.



**Equipment Used:** MiniFlex XpC

**Analysis Method:** Graphitization analysis





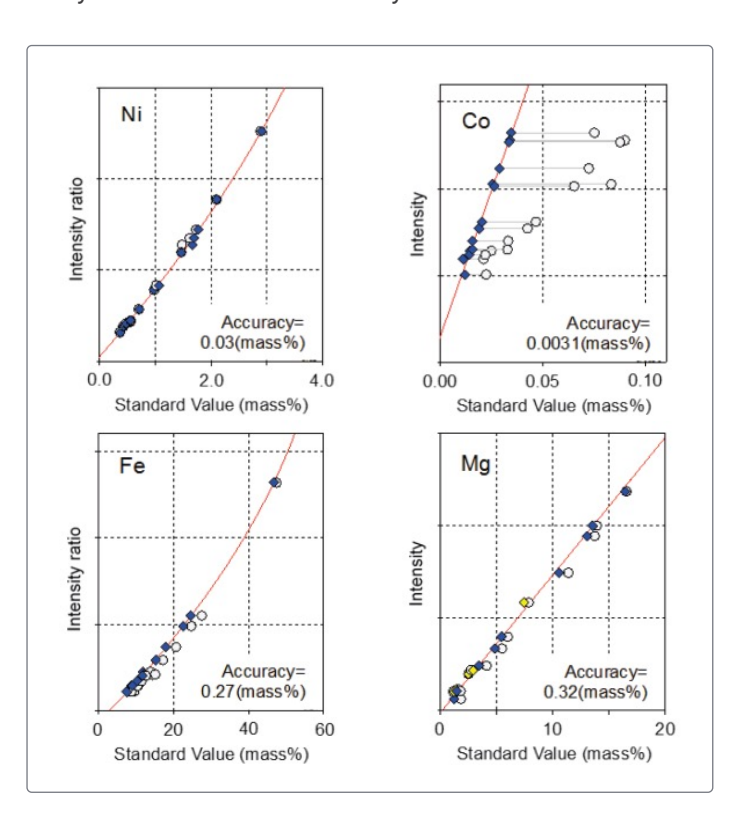
### **Composition Analysis for Nickel Laterite**

**Analysis:** Raw materials **Use:** Quality assurance

Analyzed materials: Nickel laterite

Composition analysis

In nickel-laterite minerals, accurate quantitative analysis is required for Ni and Co, which determine ore grade, as well as for Fe and Mg, which serve as indicators for determining mineral refining methods. In quantitative analysis for these elements, ICP analysis is generally used. However, using XRF analysis makes it possible to perform similar analysis faster and more readily.



Elements	Standard Conc.	Analysis Conc.
Ni	1.02	1.01
Со	0.0899	0.0873
Fe	25.57	27.88
Mg	1.81	1.91

Table 1: Composition analysis results using XRF

**Figure 1:** Calibration curve according to the powder press method for nickel-laterite mineral standard samples

**Conclusion:** Through matrix correction combining the Compton scattering internal standardization method and FP method, a highly accurate calibration curve was obtained. Additionally, analysis concentrations were nearly consistent with standard concentrations. It is possible to swiftly obtain a highly reliable mineral composition with the materials still in powder form without acid dissolution or other complex forms of pre-treatment required for ICP analysis.



**Equipment Used:** Supermini200

Analysis Method:

Matrix correction calibration curve





### Main Component Analysis for NCM Cathode Material

Analysis: materials

Processed

Analyzed materials: Li(Ni,Co,Mn,)O,

Use: Quality assurance

In NCM cathodes, Ni, Co, and Mn composition is a key factor in determining battery properties. ICP analysis is generally used to determine composition. However, sample preparations, such as acid dissolution, and dilution are necessary. With XRF, it is possible to swiftly and readily perform analysis with the materials still in powder form. Additionally, with the standardless FP method, precise composition analysis can be performed without preparing standard samples or a calibration curve.

Sample		Ni	Со	Mn
Sample A	Analysis Value	0.332	0.326	0.342
NCM (0.33/0.33/0.34)	ICP	0.33	0.33	0.33
Sample B	Analysis Value	0.847	0.098	0.055
NCM (0.85/0.10/0.05)	ICP	0.85	0.10	0.05
Sample C	Analysis Value	0.507	0.198	0.295
NCM (0.5/0.2/0.3)	ICP	0.50	0.20	0.30

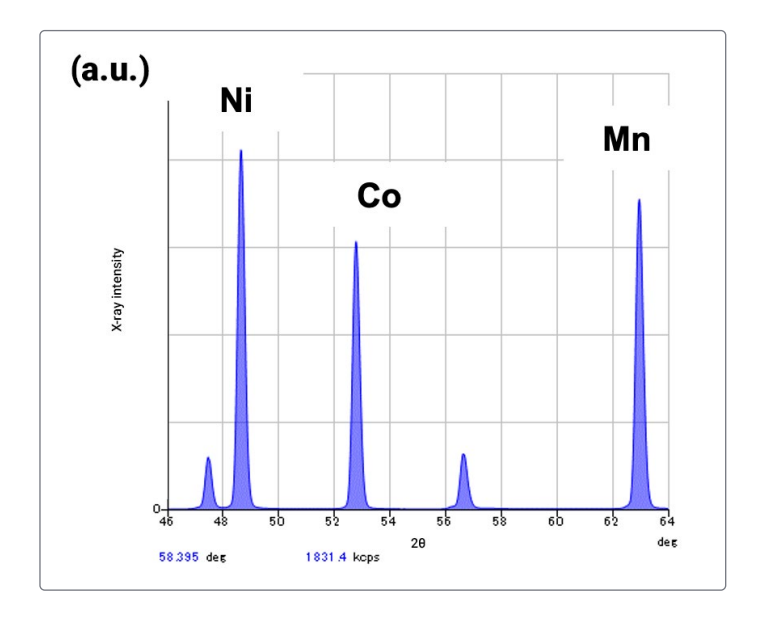


**Table 1:** Standardless FP analysis results for powder (Molar ratio)

Figure 1: Spectrum

**Conclusion:** Ni, Co, and Mn ratios in NCM obtained through the standardless FP analysis method were shown to be consistent with those from ICP analysis. It is possible to obtain similar results in an electrode status as well as powders, which is commonly used for elemental analysis. With XRF analysis, the preparation of a calibration curve and sample preparation steps such as acid dissolution and dilution, which are required in ICP analysis, are not necessary. For that reason, XRF analysis makes it possible to significantly reduce running costs and work times.



**Equipment Used:** Supermini200





### **Impurity Analysis for NCM Cathode Material**

Analysis: Processed An

materials **Use:** Quality assurance

Analyzed materials: Li(Ni<sub>2</sub>Co<sub>2</sub>Mn<sub>2</sub>)O<sub>2</sub>

Trace impurities inside cathode active materials affect battery properties and are a factor that causes degradation. Even trace Na and Mg impurities that are difficult to analyze with energy dispersive X-ray fluorescence (EDXRF) can be analyzed with precision using wavelength dispersive X-ray fluorescence (WDXRF). Additionally, with the standardless FP analysis method, it is possible to analyze from ppm levels of light to heavy elements up to 100% without preparing a calibration curve using standard samples.

(nnm)

						(ppm)
	Na	Mg	Al	Si	Ca	Fe
А	201	152	14915	291	ND	66
В	61	ND	40	339	ND	80
С	61	17	31	115	ND	87
D	160	44	50	258	54	145
Е	227	79	164	381	44	21
F	655	30	1119	256	11	104
G	152	72	57	361	86	112
Н	300	68	43	246	118	118
1	330	75	51	428	43	24
J	256	63	36	454	97	97

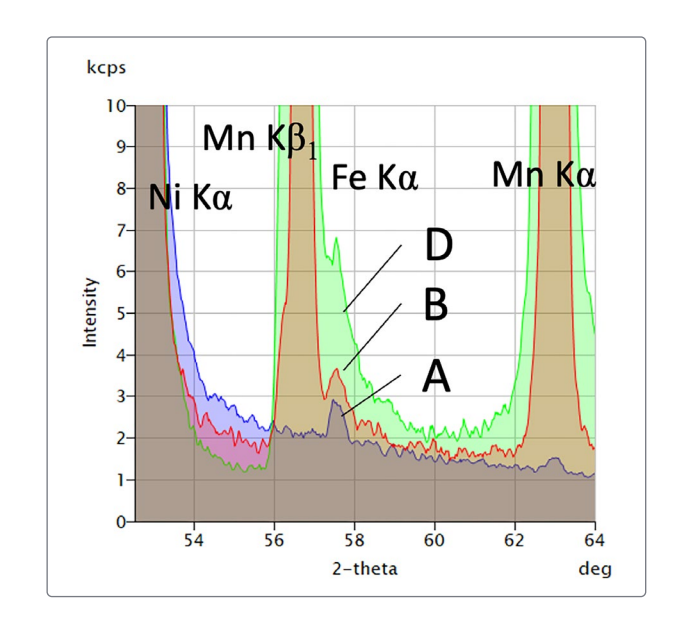


**Table 1:** Standardless FP analysis results for NCM powder samples A to J

Figure 1: Fe spectrum based on WDXRF

**Conclusion:** Na, Mg, Al, Si, Ca, Fe and other impurities were detected. Because Fe and Mn can be separated, it is possible to analyze the peak of trace Fe impurities.

Compared to EDXRF, WDXRF has higher energy resolution and is less prone to being affected by interfering lines, making it possible to obtain high sensitivity even with light elements such as Na and Mg. As such, with WDXRF, highly reliable analysis values can be obtained for a wide range of elements.



**Equipment Used:** ZSX Primus IV





### **Impurity Analysis for Graphite Anodes**

Analysis:

Processed

**Analyzed materials:** Graphite anodes

materials **Use:** 0

Quality assurance

In impurity control for graphite, which is used as an anode, XRF enables element analysis on ppm order in a non-destructive manner with the material still in powder form. Even trace Na and Mg impurities that are difficult to analyze with energy dispersive X-ray fluorescence (EDXRF) can be analyzed with precision using wavelength dispersive X-ray fluorescence (WDXRF).

(ppm)

Sample	Na	Na Mg		Na Mg Al		S	Ca	Fe	Zr
А	83	249	28	38	73	39	13		
В	N.D.	975	24	2958	41	6	N.D.		
С	81	242	42	76	81	180	4		





**Figure 1:** Sample preparation using loose powder method with commercially available graphite samples

**Conclusion:** A considerable amount of high-concentration S impurity components were detected in Sample B. A considerable amount of Fe impurity components were detected in Sample C. XRF analysis enables measurement with simple sample preparation that consists solely of filling the container with sample powder.

Compared to EDXRF, WDXRF has higher energy resolution and is less prone to being affected by interfering lines, making it possible to obtain high sensitivity even with light elements such as Na and Mg. As such, with WDXRF, highly reliable analysis values can be obtained for a wide range of elements.



**Equipment Used:** ZSX Primus IV





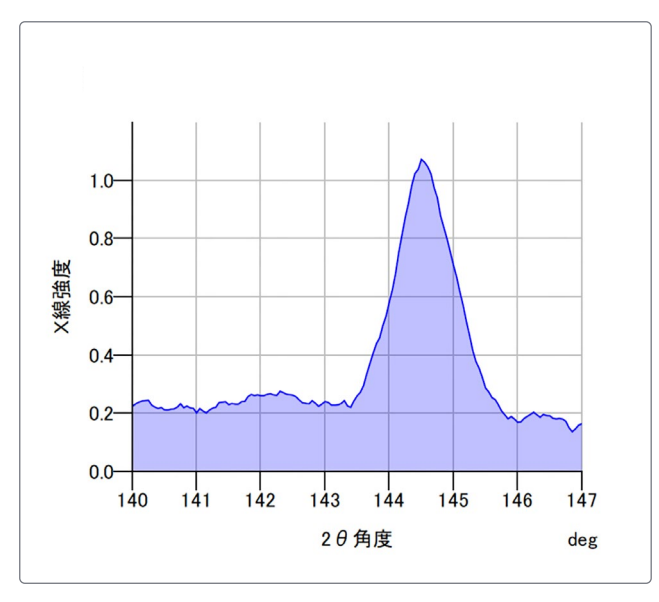
### Impurity Analysis for Silicon Metal Anode Material

Analysis: Recycled Analyzed materials: Si metal anodes

Use: Screening

Si metals, which are used as anodes, are often recycled from silicon wafer scrap. As such, they require impurity control upon acceptance. With the X-ray fluorescence analysis method, it is possible to nondestructively analyze elements at ppm level with the material still in powder form. Even AI impurities in Si matrices, which present difficulties with energy dispersive X-ray fluorescence (EDXRF), can be analyzed with precision using wavelength dispersive X-ray fluorescence (WDXRF).

#### **WDXRF**



#### **EDXRF**

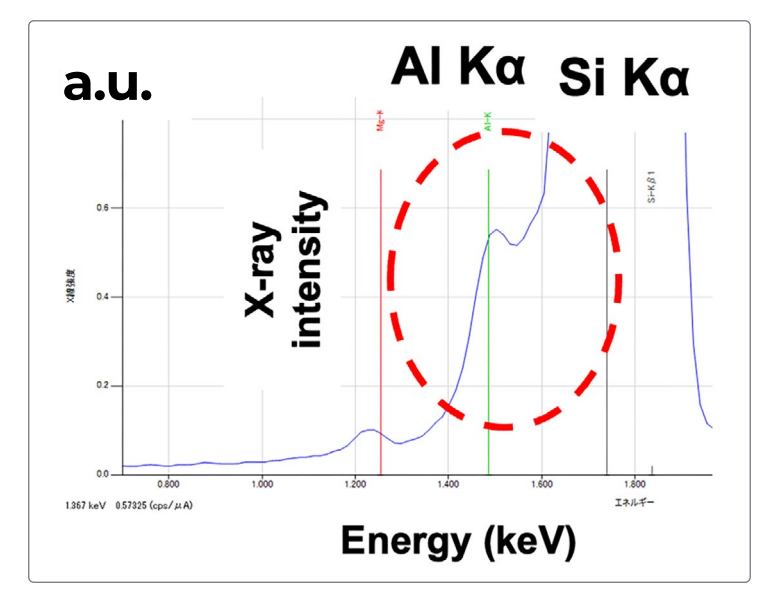


Figure 1: Al spectrum comparison of WDXRF and EDXRF

Elements			Ca (ppm)		
Analysis Value	1754	832	270		

**Table 1:** Standardless FP analysis results for electrode grade Si powder

**Conclusion:** Al, Fe, and Ca impurities were detected by XRF analysis. On the EDXRF spectrum, the Al peak overlaps with the Si peak. On the WDXRF spectrum, however, it is possible to obtain an Al peak without overlap, making trace analysis possible.



**Equipment Used:** Supermini200

Analysis Method:
Matrix correction calibration curve





### Verification of Winding Misalignment and Anode Overhang Analysis for Lithium-Ion Battery Winding Body

**Analysis:** Whole battery **Use:** Quality assurance

**Analyzed materials:** 

18650-type Lithium-ion batteries

→ Non-destructive imaging

To prevent abnormal heating in lithium-ion battery cells, it is important to verify the misalignment of winding and assess the anode overhang in the winding body during the manufacturing process. In these assessments, two-dimensional X-ray fluoroscopes are generally used. However, this only yields assessments from a single planar direction and does not allow for assessments of entire samples in three dimensions. X-ray CT allows the state of the insides of samples to be observed in a non-destructive manner. It also enables length measurements of entire samples and quantitative assessments of the shape of each material using analysis software.



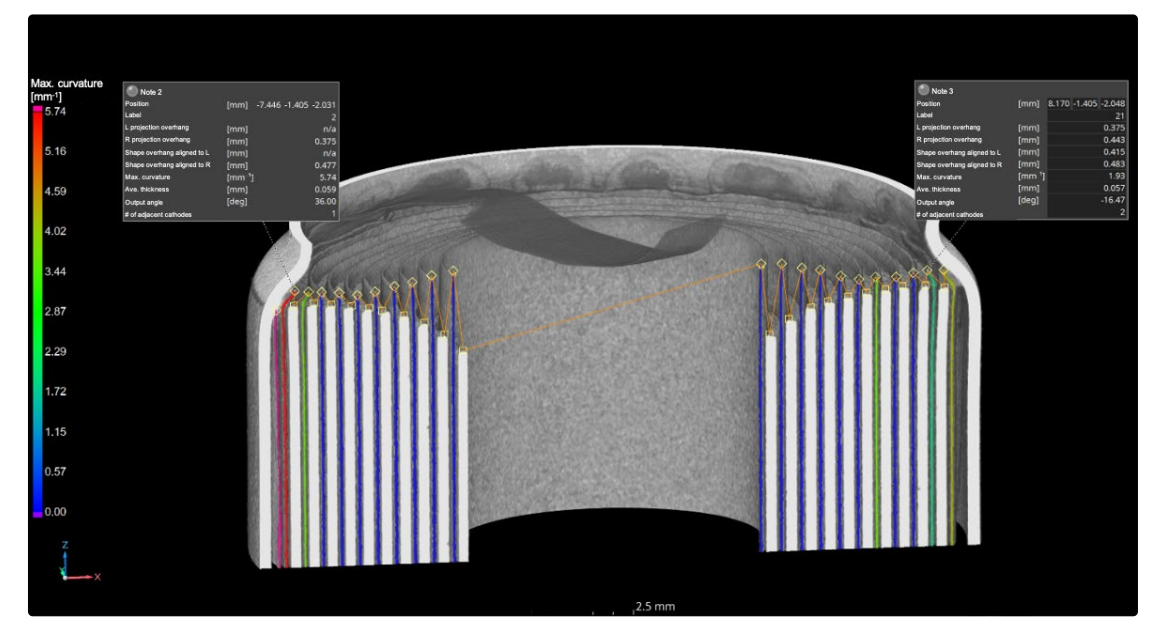


**Figure 1:** Cross-section image

Figure 2: Anode overhang analysis

**Conclusion:** A CT scan was taken of the entirety of an 18650-type lithium-ion battery. Anode overhang analysis was then performed. This made it possible to verify the presence of considerable misalignment of winding between the interior and exterior of the winding body, as well as a high curvature on the anode outside of the battery cell. A review of calendaring conditions and enclosing size of the winding body, etc. can be examined based on these results.



**Equipment Used:** CT Lab HV

**Analysis Method:** VGSTUDIO MAX





# Investigation of Phase Transition Behavior upon Cathode Material NCM Firing

Analysis: Cathode material Analyzed materials: Use: Optimizing electrochemical performance Li(Ni, Co, Mn, O), NCM

**Trystal phase analysis** 

Cathode materials are known for being synthesizable through firing using the solid-phase method. With in-situ XRD measurement, it is possible to investigate the firing process in detail by performing measurements while increasing the temperature of the samples.

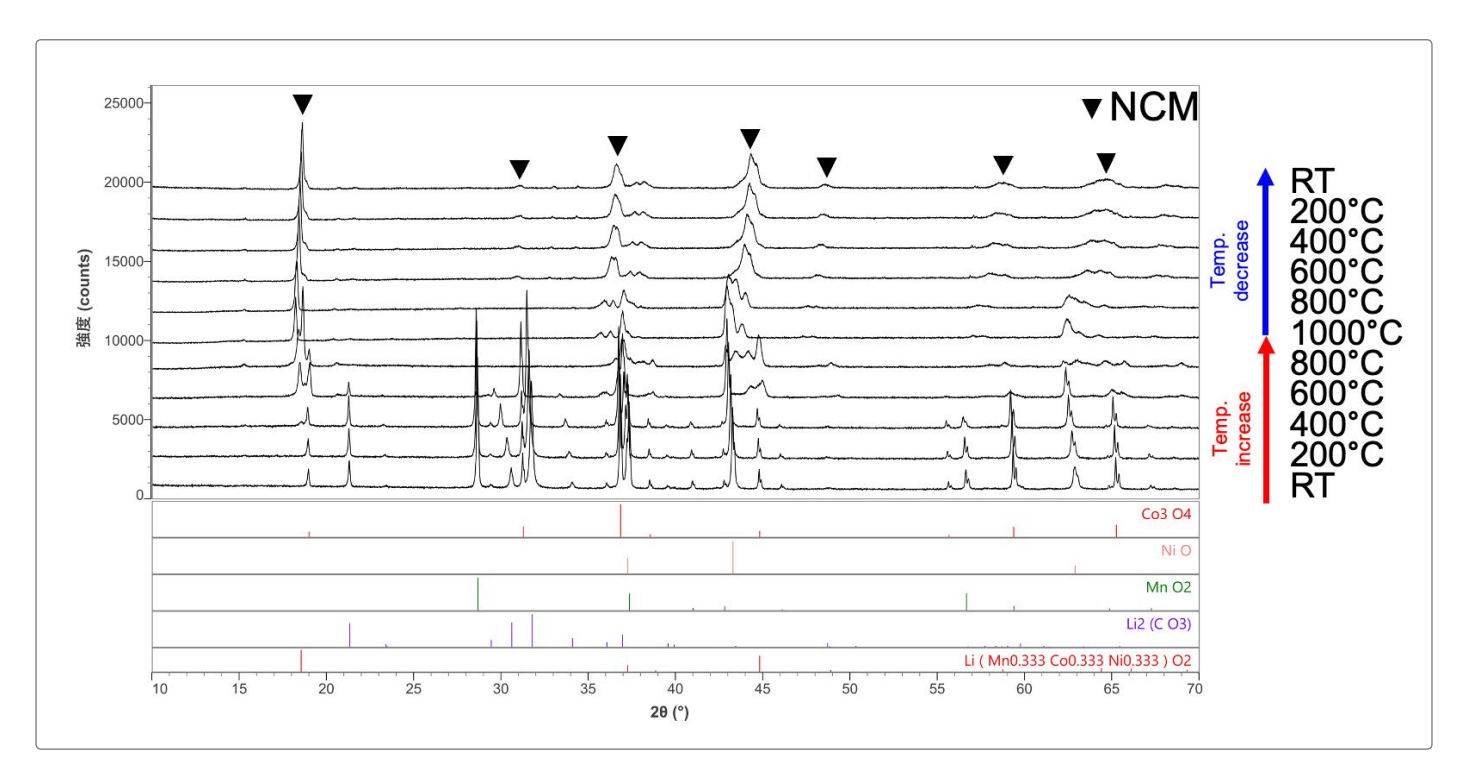


**Figure 1:** XRD profile at various temperatures (The raw material powder reacts from 600°C and becomes NCM units at 1000°C)

**Conclusion:** It is possible to capture a solid-state reaction during the sintering process. By examining firing conditions in this fashion, appropriate temperatures and times can be determined.



**Equipment Used:**SmartLab SE, SmartLab

**Analysis Method:** Qualitative analysis





# Measurement of Cathode Material NCM Using XSPA-400 ER High-Energy Resolution Detector

Analysis: Cathode material Analyzed materials: Use: Optimizing electrochemical performance Li(Ni<sub>x</sub>Co<sub>y</sub>Mn<sub>z</sub>)O<sub>2</sub>, NCM

Crystal phase analysis

In XRD using Cu radiation sources, peak profile backgrounds for cathode materials are generally high due to the effects of the transition metal elements they contain. This makes the detection of trace crystal phase peaks difficult. The XSPA-400 ER uses high energy resolution to decrease X-ray fluorescence originating from samples and reduce background components to achieve higher-sensitivity measurements compared to traditional detectors.

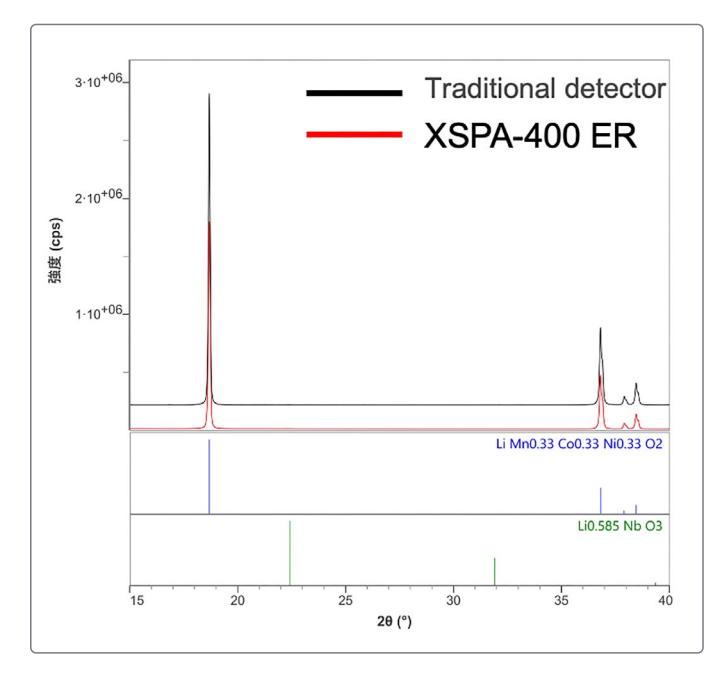


**Figure 1:** Profile measured using traditional detector and XSPA-400 ER

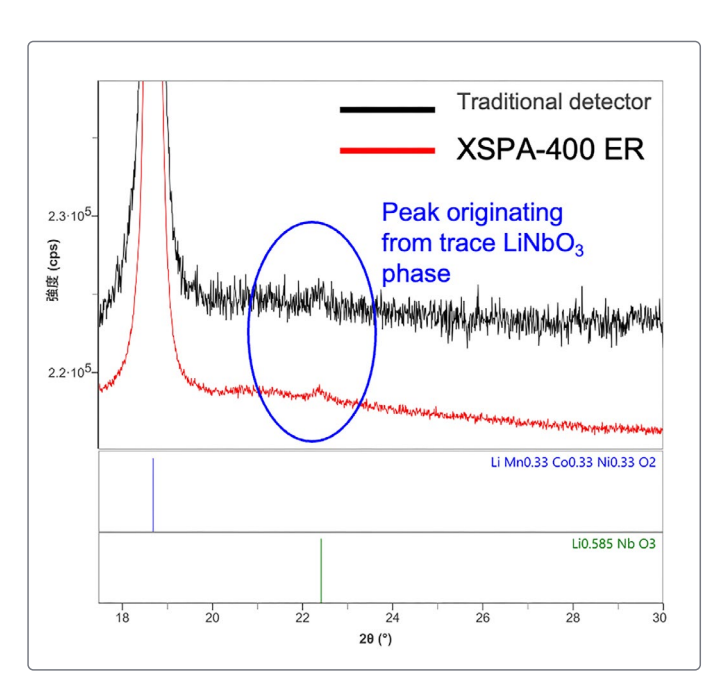


**Figure 2:** Magnified XRD profile measured using traditional detector and XSPA-400 ER

**Conclusion:** The XSPA-400 ER successfully lowers background compared to traditional detectors. As such, it makes it easier to observe minute peaks, which means trace crystal phases can be observed.







# Inference of Valence and Li Ion Diffusion Path Using the BVS Method

**Analysis:** Cathode material

Optimizing electrochemical performance

Analyzed materials: LiFePO<sub>4</sub>, LFP

**Trystal phase analysis** 

Use:

The valence of general cathode materials affects battery performance. For that reason, they are analyzed using XAFS and ESCA. Using the BVS method, it is possible to infer valence based on interatomic distances with XRD. Additionally, by applying the BVS method it is possible to infer the diffusion path by determining the interatomic distance at which it is easy for Li ions to become monovalent.

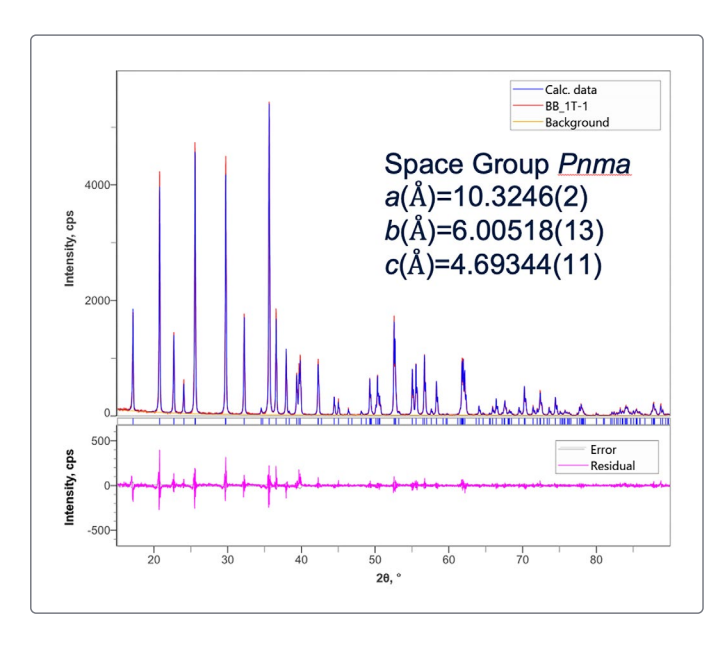


**Figure 1:** Rietveld analysis results for LFP and lattice constants obtained  $(R_{WP}:11.13\%, S:1.33)$ 

Atoms	X	У	Z	Valence According to BVS Method		
Li1	0	0	0	0.98		
Fe1	0.28231(9)	0.25	0.9744(3)	1.91		

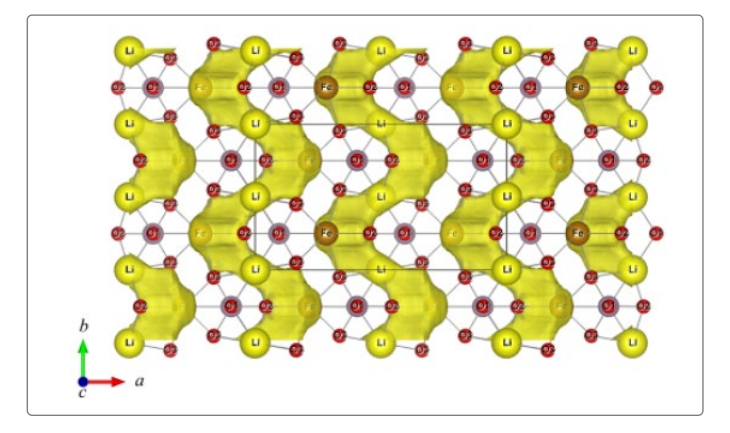


Figure 2: Li and Fe coordinates obtained using Rietveld analysis and valence obtained using the BVS method (top) and Li ion diffusion path inferred using the BVS method (bottom)

Rendered using VESTA, K. Momma and F. Izumi, "VESTA 3 for threedimensional visualization of crystal, volumetric and morphology data," J. Appl. Crystallogr., 44, 1272-1276 (2011).

**Conclusion:** Rietveld analysis makes it possible to perform structural analysis. Additionally, using the BVS method, valence and the Li ion diffusion path can be inferred.



**Equipment Used:** SmartLab SE, SmartLab

**Analysis Method:** Rietveld analysis, BVS method





# Crystallite Diameter and Particle Diameter Calculation for Silicon Negative Electrode Material

**Analysis:** Anode material **Use:** Improving battery lifetime

**Analyzed materials:** 

Si

**Trystal phase analysis** 

Anode material Si is a high-capacity material. To improve battery life, the particle diameter must be kept to no more than several dozen nm. In cases involving a diameter of 100 nm or less, the crystallite diameter can be calculated with XRD and the particle diameter can be calculated with SAXS (small-angle X-ray scattering).

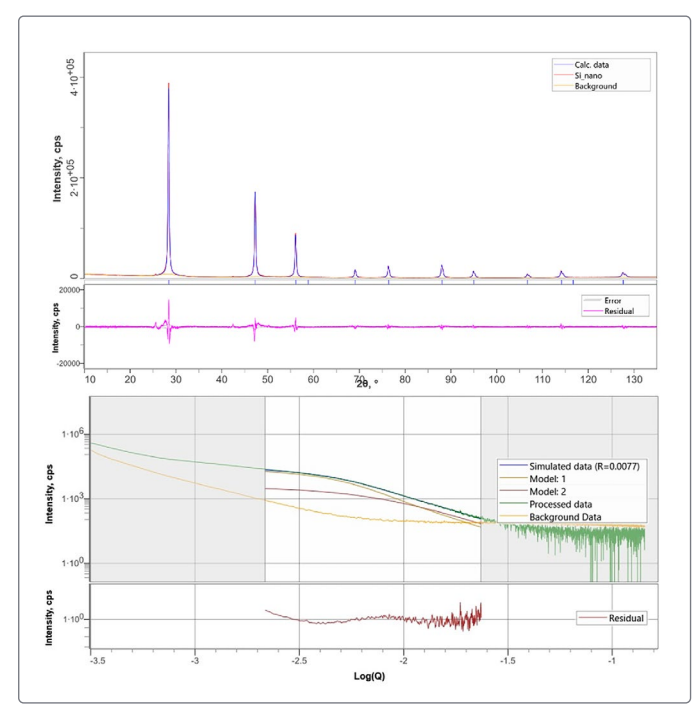
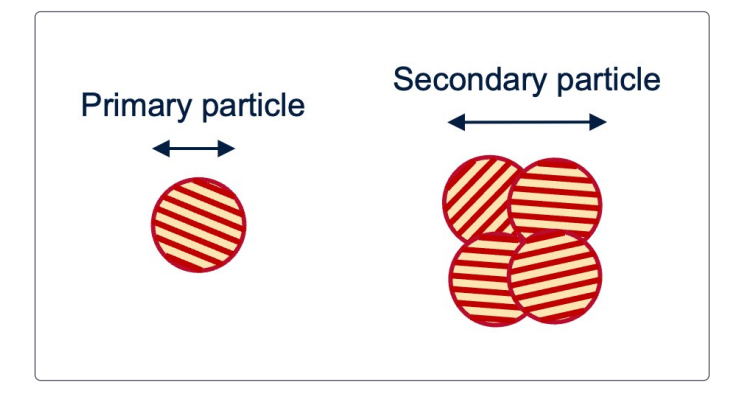


Figure 1: XRD profile (top) and SAXS profile (bottom) for Si samples



Sample	D(nm)
Crystallite diameter (XRD)	40.4
Primary particle diameter (SAXS)	39.6
Secondary particle diameter (SAXS)	82.1

**Figure 2:** Crystallite diameter and particle diameter (It was verified that the crystallite diameter and primary particle are equivalent and that a secondary particle is present)

**Conclusion:** When measuring crystallite and particle diameters in the range of several dozen nm, such as those in Si anodes, methods using XRD and SAXS are optimal.



### **Equipment Used:**

NANOPIX mini, MiniFlex

### **Analysis Method:**

Crystallite size analysis using FP method and model fitting using small-angle X-ray scattering





# Measurement of $\text{Li}_7\text{P}_3\text{S}_1$ Solid-State Electrolyte Using Airtight Sample Holder

Analysis: Solid-state Analyzed materials: Li<sub>7</sub>P<sub>3</sub>S<sub>11</sub>, LPS

**Use:** Improving ionic conductivity

LPS, a sulfide solid electrolyte with high electrical conductivity, is known to readily react with moisture in the air. For hygroscopic samples like this, using an airtight sample holder enables XRD measurement without exposing the material to water in the air.

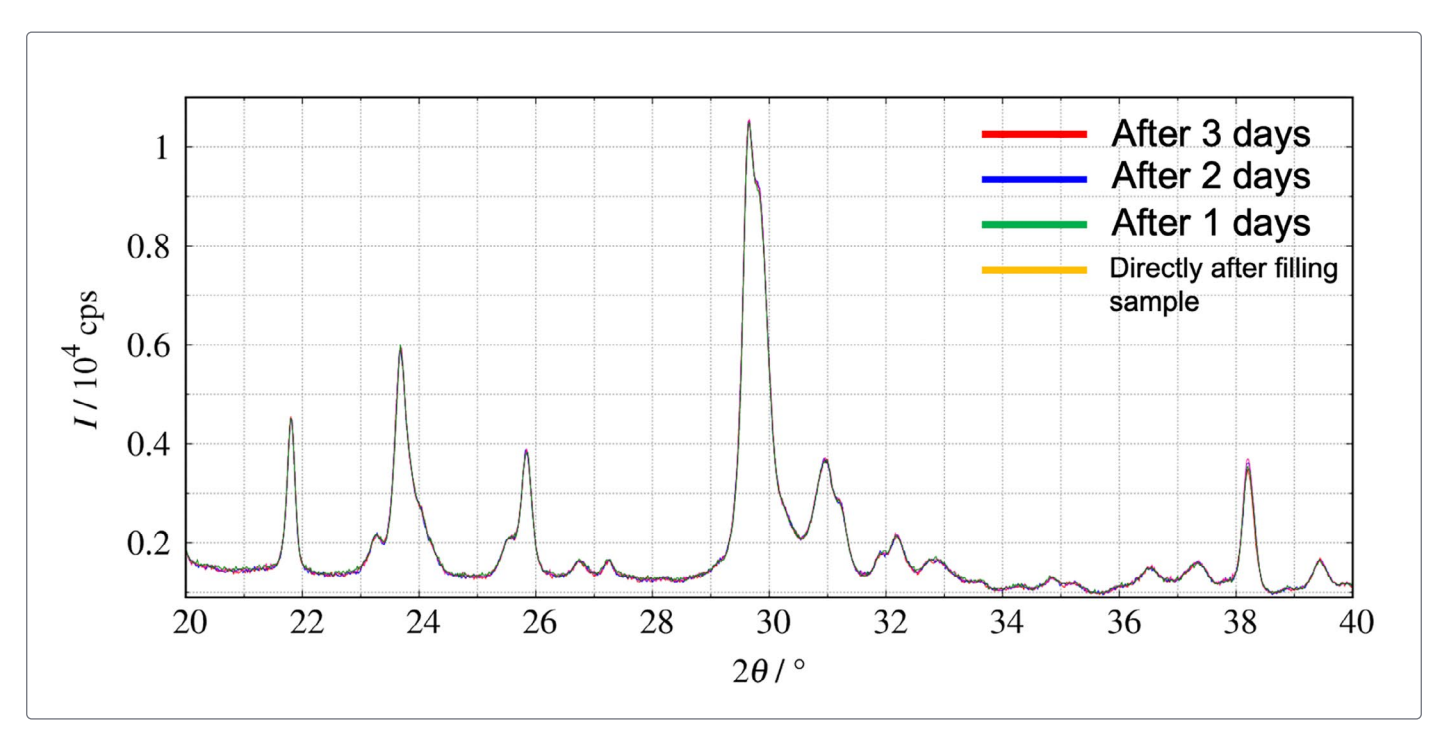


Figure 1: XRD profile for LPS

(Samples provided by: Hayashi Laboratory, Osaka Metropolitan University)

**Conclusion:** It was demonstrated that, by using an airtight sample holder, the XRD profile of LPS was unaffected by water in the air, exhibiting no change over a four-day period. Airtight sample holders are an ideal tool for verifying the synthesis of samples for which airtightness is required.



**Equipment Used:** MiniFlex, airtight sample holder

**Airtight sample holder:** US patent 11,525,790





### Local Structure Analysis of Li<sub>3</sub>PS<sub>4</sub> Solid-State Electrolyte

Analysis: Solid-state electrolytes Analyzed materials: Li<sub>2</sub>PS<sub>4</sub>, LPS

**Use:** Improving ionic conductivity

The crystalline structure of LPS is known to be related to its Li ion electric conductivity. However, as LPS exhibits low crystallinity near room temperature, applying traditional structural analysis methods, such as Rietveld analysis, proves difficult. Meanwhile, pair distribution function (PDF) analysis can analyze local atomic structures even with non-crystalline materials. For that reason, PDF analysis combined with the RMC (Reverse Monte Carlo) method was applied to investigate how LPS's disordered crystal structure relates to electric conductivity at varying temperatures. For details, please refer to the cited papers.

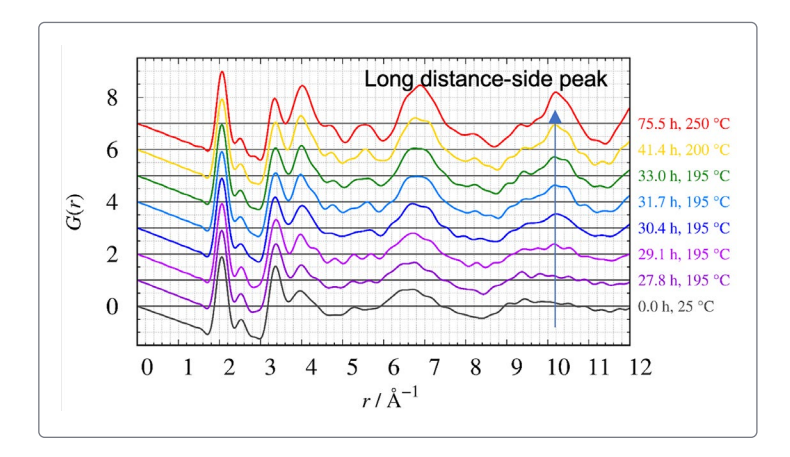


**Figure 1:** PDF analysis results obtained for each room temperature and retention time (y-axis: G(r); x-axis: interatomic distance)

When temperature rises, a long distance-side peak in interatomic distance is visible. As such, crystallization can be ascertained to be taking place.

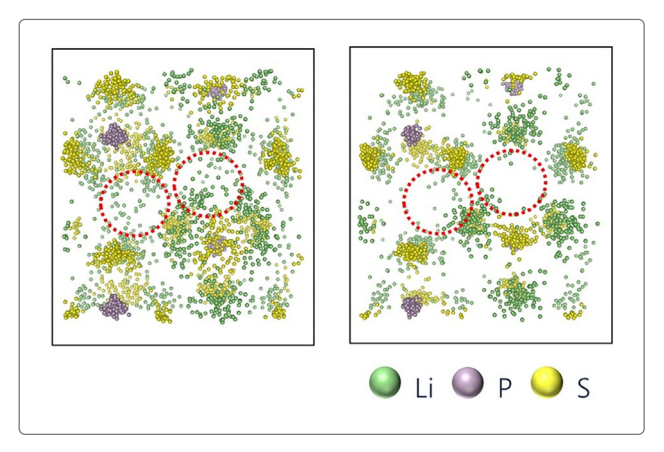


Figure 2: Crystalline structure at room temperature (298K) and 523K obtained through RMC method

It can be ascertained that the distribution of Li expands from the local structure circled above to a glass state.

**Conclusion:** By applying the RMC method using PDF analysis, which can be applied even to non-crystalline material, each crystal state can be analyzed.

\*Cited papers M. Yoshimoto, T. Kimura, A. Sakuda, C. Hotehama, Y. Shiramata, A. Hayashi, K. Omote, Solid State Ionics, 401 (2023), 116361 (8pp).



**Equipment Used:** SmartLab

**Analysis Method:** PDF analysis, RMC method





# XRD Measurement During Charge/Discharge Using Laminated Cell Batteries

Analysis: Whole battery

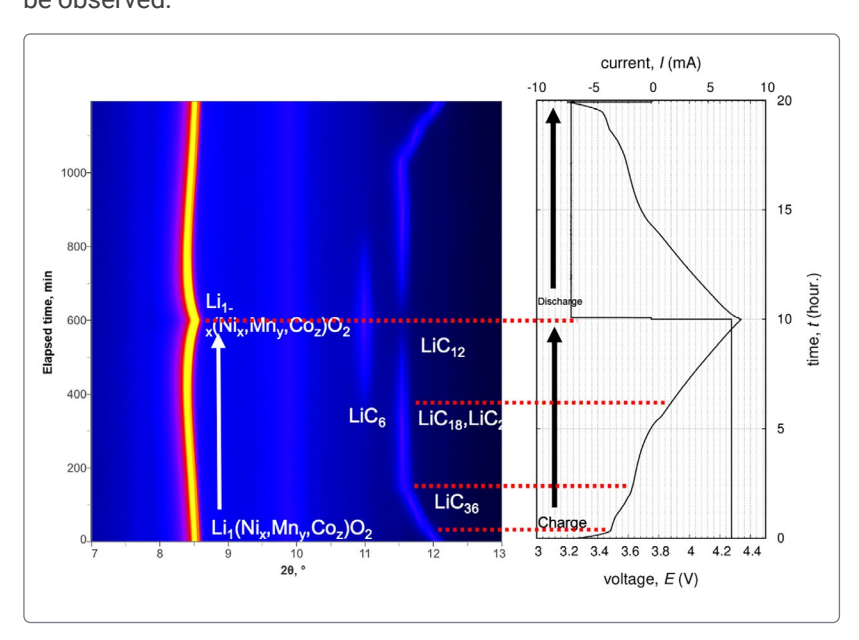
**Use:** Improving battery performance

Phase transition analysis

**Analyzed materials:** Laminated cell batteries

(Cathode NCM, anode C, separator, electrolyte solution)

With operando measurement, in which XRD measurement is conducted while charging/discharging, crystal phase transition behavior during charge/discharge can be ascertained. This can be used to clarify charging/discharging mechanisms and estimate battery capacity deterioration. Additionally, since measurement of laminated cell batteries is generally conducted using the transmission method, information about both positive and negative electrodes can be observed.



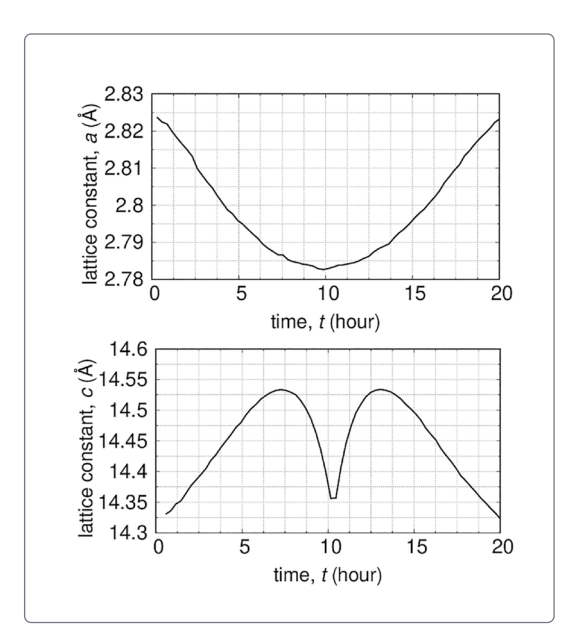


**Figure 1:** Observations of change in lattice constant (elapsed time vs  $2\theta$  (left) and charge/discharge profile (right), NCM) and observations of changes in crystalline structure (C)

Figure 2: Change in a-axis and c-axis for NCM

**Conclusion:** Changes in the lattice constant upon charging/discharging were successfully observed with operando measurement using laminated cell batteries.



**Equipment Used:** SmartLab

**Analysis Method:** Rietveld analysis, operando





# XRD Measurement during Charge/Discharge Using All-Solid-State Batteries

**Analysis:** Whole battery

**Use:** Improving battery performance

Phase transition analysis

**Analyzed materials:** 

All-solid-state Na ion batteries

(Cathode TiS2, solid-state electrolyte Na3PS4, anodes)

All-solid-state Na ion batteries are next-generation batteries that are expected to be less expensive than Li ion batteries and have faster charge/discharge performance. When operating all-solid-state batteries, it is necessary to continue applying pressure to make it easier for the ions to move within the solid. With this measurement, using cells that can be charged/discharged while applying pressure to an all-solid-state battery, the behavior of an all-solid-state Na ion battery was verified.

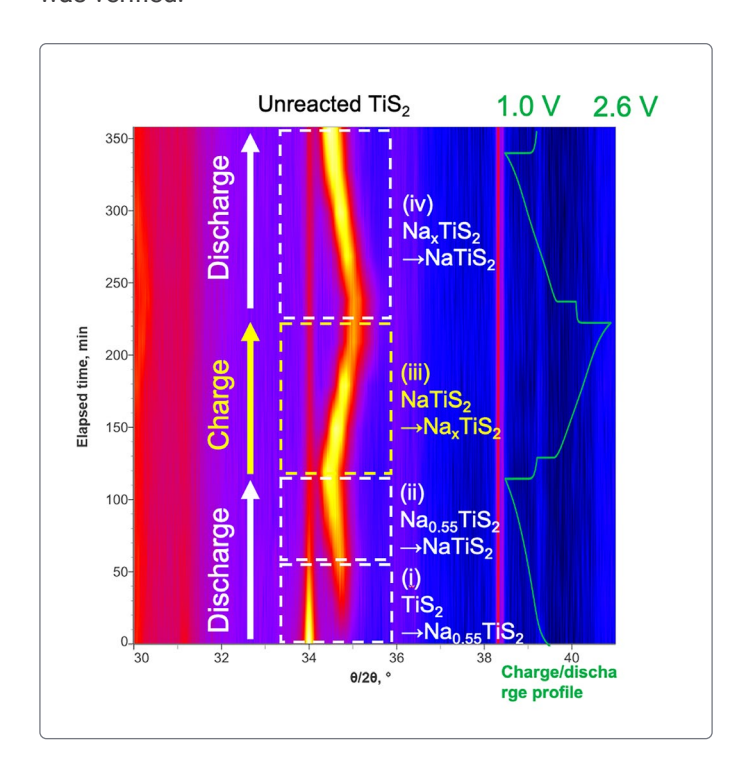


**Figure 1:** Elapsed time vs  $2\theta$  and charge/discharge profile (inside image)

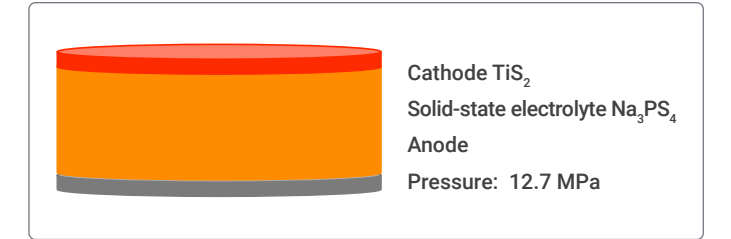


**Figure 2:** Representation of solid-state battery pellet and pressure conditions

Cathode TiS<sub>2</sub> exhibited the following changes during charging/discharging.

Phase transition from  $TiS_2 \rightarrow Na_{0.55}TiS_2$ 

- (i) Change in lattice constant from Na<sub>0.55</sub>TiS<sub>2</sub> → NaTiS<sub>2</sub>
- (ii) Change in lattice constant from NaTiS<sub>2</sub> → Na<sub>x</sub>TiS<sub>2</sub>(x < 0.55)</li>
- (iii) Change in lattice constant from Na<sub>x</sub>TiS<sub>2</sub> → NaTiS<sub>2</sub>
- (iv) Unreacted TiS<sub>2</sub> was partially present

**Conclusion:** It is possible to measure changes in the crystal phase and lattice constant during charging/discharging in an all-solid-state battery.



### **Equipment Used:**

SmartLab, all-solid-state battery cells

### **Analysis Method:**

Operando measurement





# XRD Measurement with Temperature Control and Charge/Discharge Using Laminated Cells

**Analysis:** Whole battery

**Use:** Improving battery performance

Phase transition analysis

**Analyzed materials:** 

Laminated cell

(Cathode LiMn<sub>2</sub>O<sub>4</sub>,LMO, anode C, separator, electrolyte solution)

With car-mounted batteries, etc. used in an environment with assumed temperature changes, stability in the crystal phases upon charging/discharging is required at each temperature. With an attachment that enables the implementation of XRD while charging/discharging and modifying temperatures while doing so, it became possible to verify crystal phase behavior.

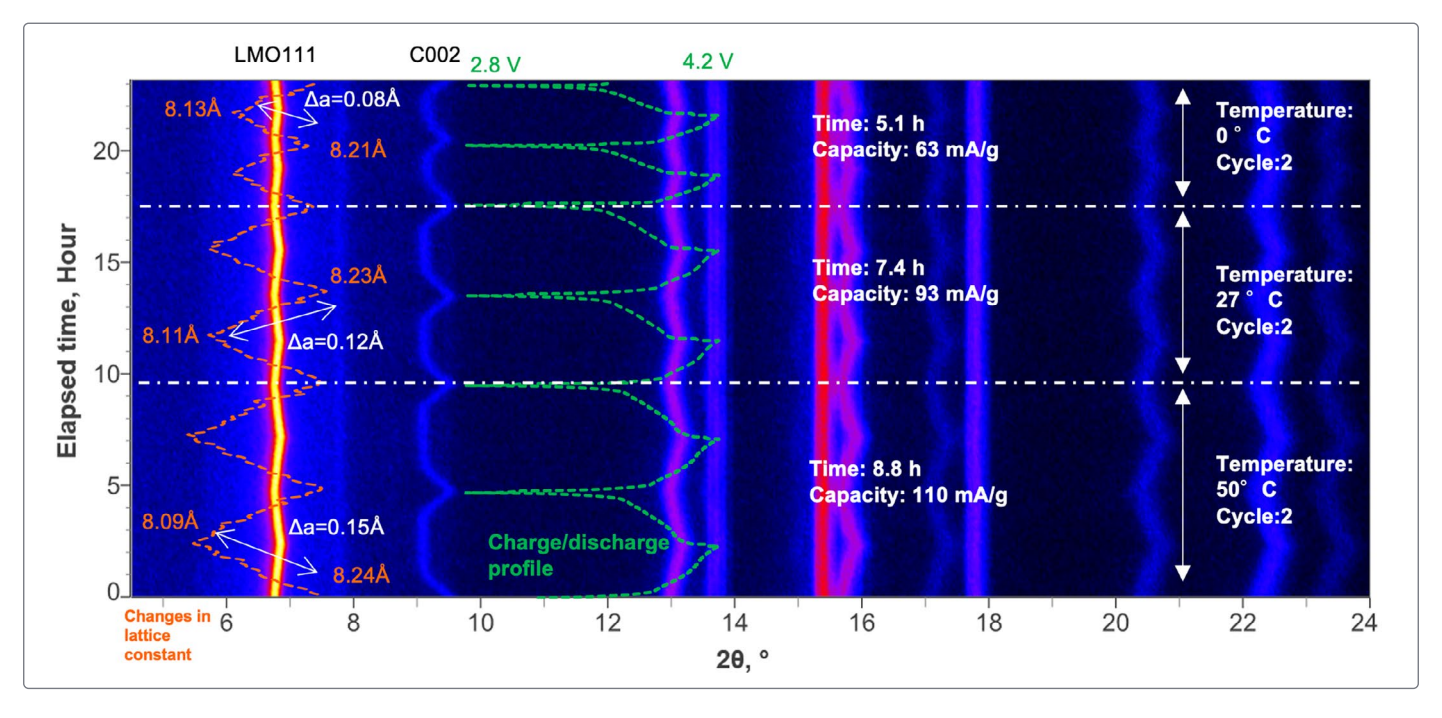


**Figure 1:** Elapsed time vs 2θ, charge/discharge profile and changes in lattice constant (inside image)

As the temperature goes from high to low, the battery capacity decreases. Accompanying this, the difference in changes in the lattice constant as indicated by  $\Delta a$  has become smaller. It can therefore be surmised that the Li ions are exhibiting less movement.

**Conclusion:** It is possible to measure changes in the crystal phase during charging/discharging while modifying temperature. When the temperature was lowered, changes in battery capacity were successfully verified. It could be surmised that changes in battery capacity are related to the amount of change in the lattice constant.



**Equipment Used:** SmartLab

Analysis Method: Operando measurement





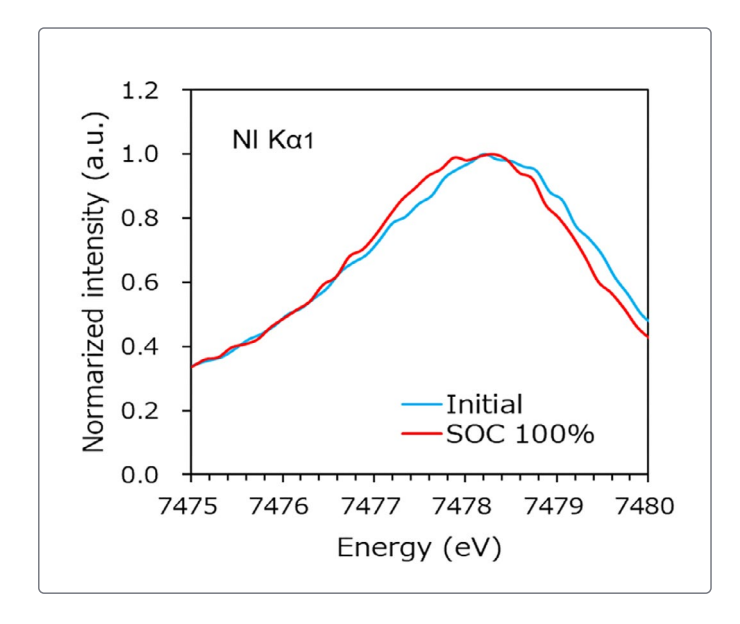
## Valence Analysis for Ni, Co, and Mn in NCM Cathodes

**Analysis:** Cathode material **Use:** Optimizing electrochemical performance

Analyzed materials: Li(Ni,Co,Mn,)O,

Chemical state analysis

Synchrotron radiation XAFS is generally used in valence analysis for transition metal elements in NCM cathodes. However, similar assessments can be performed with X-ray emission spectrometers (XES) as well. Changes in bonding state can be assessed based on chemical shifts in the XES spectrum for Ni, Co, and Mn.



0.00

()
-0.05
-0.15
-0.15
-0.20
0
50
100
SOC (%)

**Figure 1:** Ni K $\alpha$ 1 spectrum before and after charging for LiNi<sub>1/3</sub>Co<sub>1/3</sub>Mn<sub>1/3</sub>O<sub>2</sub> (NCM(111)) cathodes

**Figure 2:** Correlation between chemical shifts and state of charge for Ni Kα1, Co Kα1, and Mn Kα1

**Results:** Figure 1 illustrates the changes in the XES spectrum for Ni K $\alpha$ 1 before and after charging. Figure 2 shows changes based on the state of charge in chemical shifts for Ni K $\alpha$ 1, Co K $\alpha$ 1, and Mn K $\alpha$ 1. This correlation between chemical shifts and the state of charge can be used to estimate valence changes. As this shows, valence analysis is also possible using the XES method with laboratory instruments. Additionally, while only certain information on the surface can be analyzed with XPS, the XES method makes it possible to analyze up to a depth of several dozen  $\mu$ m with an analysis diameter of 10-20 mm.





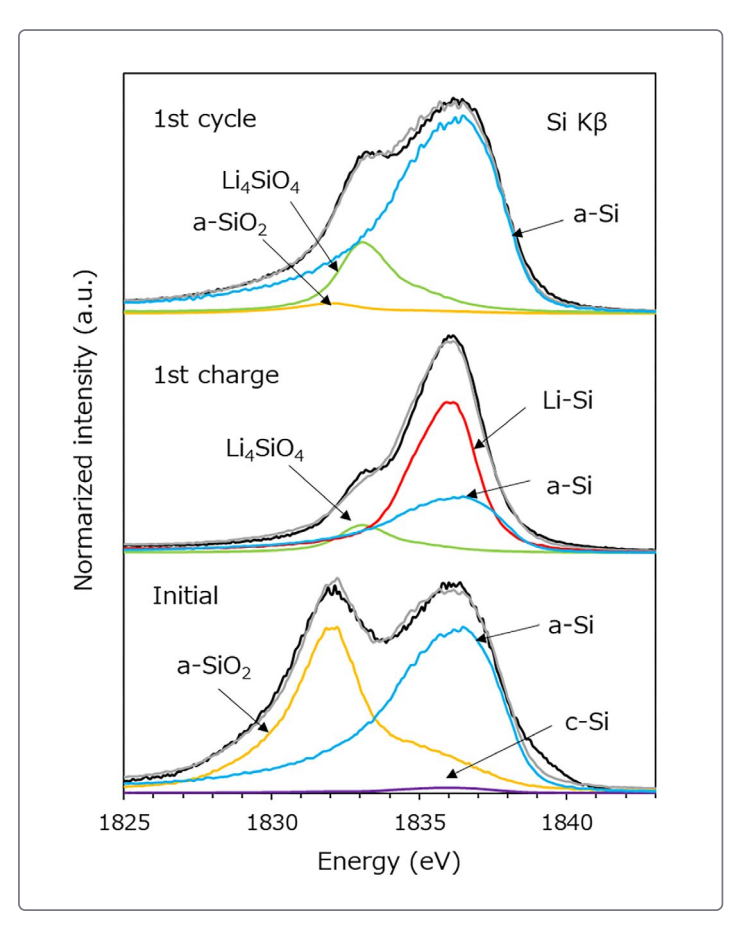
# Composition analysis of Li/Si Ratio and Silicate in Silicon Based Anodes

**Analysis:** Anode material **Use:** Improving battery lifetime

**Analyzed materials:**Si metal anodes, SiO anodes

Chemical state analysis

Synchrotron radiation XAFS is generally used in chemical state analysis for metal elements. However, similar assessments can be performed with X-ray emission spectrometers (XES) as well. XES analysis for Si can also be applied to electrode reaction analysis and degradation analysis.



This figure illustrates an XES spectrum for Si  $K\beta$  upon initial charging/discharging for SiO-C composite anodes.

Linear combination fitting (LCF) was conducted using a standard spectrum for crystal Si (c-Si), amorphous Si (a-Si), Li<sub>3.75</sub>Si (Li-Si), SiO and Li<sub>4</sub>SiO<sub>4</sub>.

**Conclusion:** When uncharged, SiO is comprised of a-Si and  $SiO_2$ . However, it was ascertained that with charging, Li-Si and  $Li_4SiO_4$  are generated, and that a-Si and  $Li_4SiO_4$  are generated after the cycle. As this shows, state analysis for compounds is also possible using the XES method with laboratory instruments.





(Unit: mol)

# Composition Analysis for Argyrodite-Based Sulfide Solid Electrolyte Material

**Analysis:** Solid state electrolyte **Use:** Improving ionic conductivity

Analyzed materials: LPSCI argyrodite

**Representation** Representation analysis

Sulfide solid electrolyte materials, of which LPS and argyrodite are leading examples, react with moisture in the air. As such, they need to be treated without exposure to the air. Composition analysis using XRF was made possible by sealing pellets inside a vacuum pouch cell. While ICP analysis is used for composition analysis, sulfur and halogen are prone to volatilization, necessitating complex pre-treatment. With XRF, analysis can be performed with material still in powder form, making for swift, convenient analysis.



This figure shows the production method for a vacuum pouch cell.

A 10 mm pellet is inserted in film and then vacuum-sealed.

				(OIIIL IIIOI)
	Synthesis conditions	P	S	Cl
	Target composition	1.00	4.50	1.50
А	Mechanochemical Milling	1.00	4.49	1.52
В	Heating for 2h at 550°C (Vacuum)	1.00	4.30	1.44
С	Heating for 6h at 450°C (Vacuum)	1.00	3.87	1.55

This table illustrates composition analysis results in synthesis conditions.

**Conclusion:** Synthesis conditions for argyrodite-based LPSCI were examined. Through a comparison with target composition, it was ascertained that at 550°C, S and CI volatilized, and that, at 450°C as well, S volatilized after being heated for a long period of time. As this shows, using XRF analysis without exposure to the air enables analysis consistent with intended composition in a short amount of time.



**Equipment Used:** ZSX Primus IV





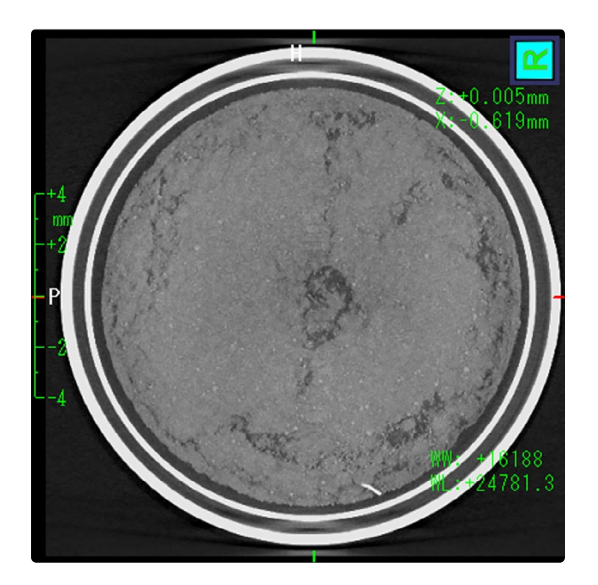
# Particle Distribution Analysis and Crack Analysis in Lithium-Ion Batteries

**Analysis:** Whole battery **Use:** Improving battery performance

**Analyzed materials:**Lithium-ion batteries CR2032

Non-destructive analysis

In the design and development of batteries, it is essential to assess the internal structures of various components and materials using prototype samples. However, when performing assessments of the internal structure of prototypes using SEM, etc., physical destruction of the sample and the preparation of an observation surface were necessary. X-ray CT enables the observation of the state of the inside of sample in a non-destructive manner. The state of parts and materials observed using analysis software can be quantitatively assessed. With this assessment, a used cointype lithium-ion battery was scanned using X-ray CT, and the crack volume generated inside the sample, the diameter of dispersed particles within and their distribution were assessed.





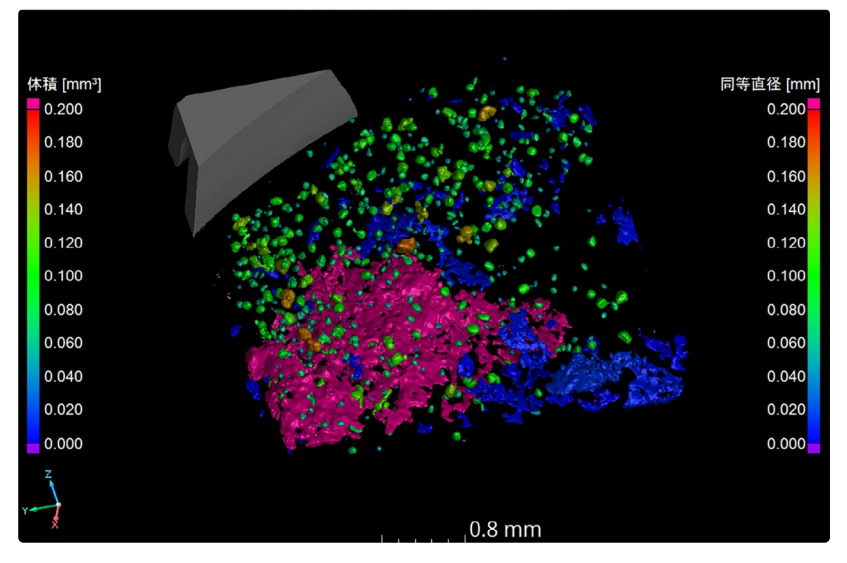


**Figure 2:** Analyzing part of crack analysis and particle diameter distribution analysis (Figure 1)

**Conclusion:** Based on Figure 1, in the sample following energization, the generation of cracks can be verified in the entire sample. Based on Figure 2, it can be ascertained that the dispersed particle diameter is roughly 0.1 mm, and that the particles are dispersed in the outer part of the sample. By observing the internal structure nondestructively, one can hypothesize where the cracks started and how their sizes relate to the distribution of the particles.







### Assessment of Particle Diameter and Interparticle Voids for Cathode Material for Lithium-Ion Batteries

**Analysis:** Cathode material Use:

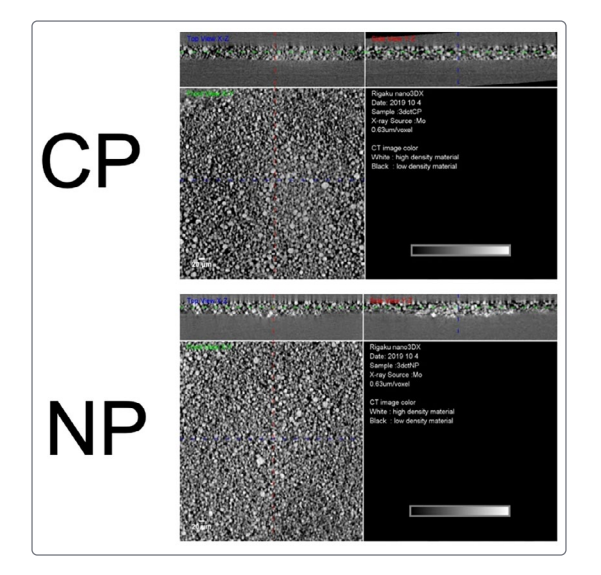
Optimizing electrochemical performance

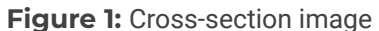
**Analyzed materials:** 

Cathode material for lithium-ion batteries

Non-destructive analysis

In the development of lithium ion-battery cathode material, the distribution of active material, their particle diameter and interparticle voids are important for the sake of improving battery capacity. In assessments of active material using SEM, etc., only surface observations of the sample are possible, and evaluations of particle size and voids within the sample are not feasible. With X-ray CT, the state of both the surface and inside test-produced cathode material can be non-destructively observed in three-dimensions, and the distribution of active material as well as particle diameters and voids can be assessed.





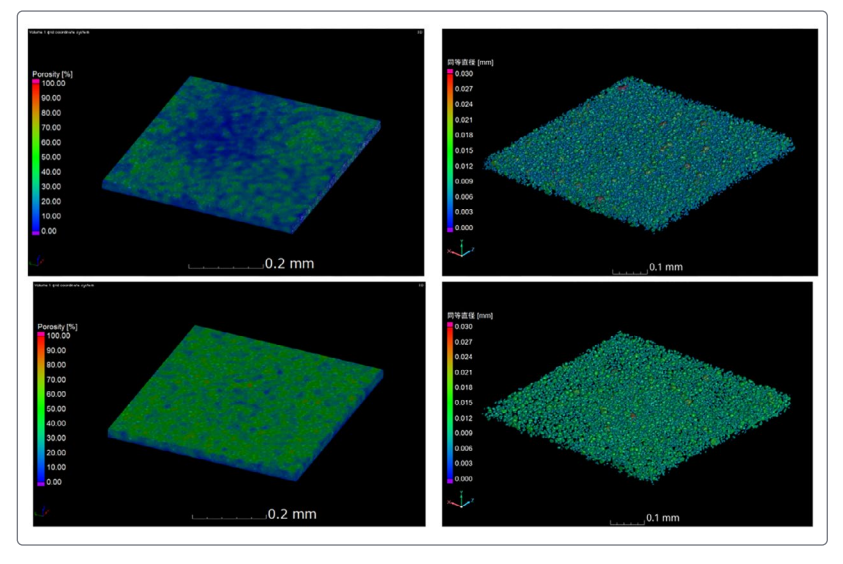


Figure 2: Assessment of interparticle voids and particle diameters in active material

Conclusion: Using two types of cathode material with differing preparation methods, the interparticle voids and particle diameters in active material were assessed. It was successfully determined that Sample CP has fewer voids than Sample NP, and that particles of varying size are dispersed in the former. By assessing battery capacity using this cathode material, it is also possible to infer the relationship between battery capacity and the interparticle voids and particle diameters of the active material.







### Thermal Stability Analysis of Separators via DSC and TMA

Analysis: Separator material Analyzed materials: Use: Evaluation of thermal stability Three-layer separator

The primary function of separators in Li-ion batteries is to prevent contact between anode and cathode while facilitating Li-ion transport through fine pores. The separators require dimensional stability within the operating temperature range and a shutdown function that collapses the pores to prevent thermal runaway. Thermomechanical Analysis (TMA) and Differential Scanning Calorimetry (DSC) are applied to characterize this performance.

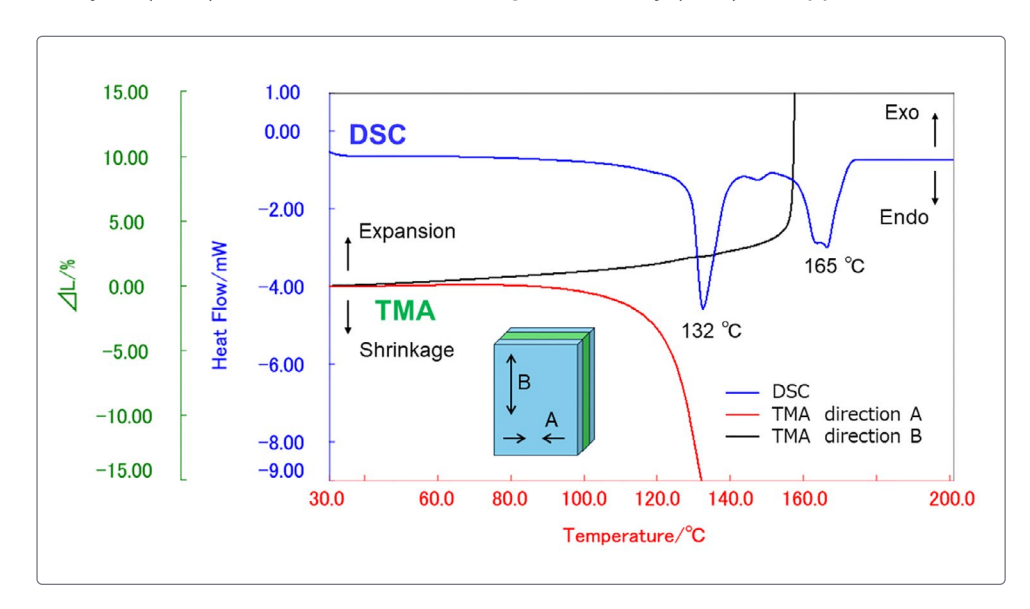


Figure 1: TMA and DSC for three-layer separator

DSC revealed endothermic peaks corresponding to the melting of polypropylene and polyethylene at 132°C and 165°C, respectively. The melting of porous polyethylene triggers the shutdown function.

With TMA, we can identify shrinkage around the polyethylene melting temperature in the A direction, while elongation occurs above the polypropylene melting temperature in the B direction.

**Conclusion:** TMA and DSC allow us to evaluate the thermal shrinkage and shutdown temperature of separators. These analyses are valuable for evaluating separator thermal stability and guiding material selection.



Equipment Used:
DSCvesta2,
TMA8311

Analysis Method:







# Accuracy Improvement of Fe/P Molar Ratio Analysis in LiFePO<sub>4</sub> Cathode Material

**Analysis:** Processed materials

Quality assurance

**Analyzed materials:** 

LiFePO,

\* Elemental Analysis

Use:

The quality of LiFePO<sub>4</sub> cathode material is closely related to battery capacity, life, and safety. In particular, molar ratio of the main component, Fe/P, is an indispensable factor for the formation of an ideal crystal structure. Even small deviation in composition can cause performance variation and degradation. In standardless FP analysis, more accurate analysis result can be obtained by registering a sample that is similar to the analyzed sample as a standard sample in the matching library.

		Sam	ple A	Sample B	Sample C
	Stoichiometric value	SQX result (w/o matching)	SQX result (matching)	SQX result (matching)	SQX result (matching)
Fe (mass%)	35.40	37.26	35.37	34.01	34.91
Theoretical Std Dev (mass%)		0.03	0.03	0.03	0.03
P (mass%)	19.64	18.56	19.62	19.64	19.81
Theoretical Std Dev (mass%)		0.02	0.02	0.02	0.02
Fe/P (mol ratio)	1.00	1.11	1.00	0.96	0.98

Table 1: MSQX analysis results of Fe and P, theoretical standard deviation and molar ratio of Fe/P

**Conclusion:** Matching library registration was performed by using sample A (LiFePO<sub>4</sub> reagent) as the standard sample. The molar ratio of Fe/P was calculated as 1.00. Slight deviations from 1.00 were observed in the molar ratio of Fe/P in the analysis results of Samples B and C, which are battery grade electrode materials. The theoretical standard deviation, which is an indication of analytical error, was about 0.03 mass% for both Fe and P, indicating that the difference between the analysis results of samples B and C and their stoichiometric values is significant. The results show that even with standardless FP method, the analysis reliability can be improved and small differences in composition can be detected quantitatively.



**Equipment Used:** ZSX Primus IV





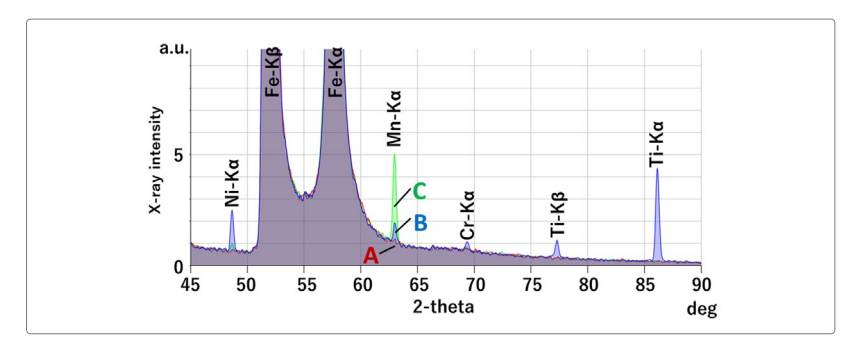
# Highly Sensitive Analysis of Trace Component on LiFePO<sub>4</sub> Cathode Material

Analysis: Cathode material Analyzed materials:

**Use:** Optimizing electrochemical performance LiFePO<sub>4</sub>

\* Elemental Analysis

LiFePO<sub>4</sub> cathode active materials contain trace components resulting from raw materials, impurities from the manufacturing process, which may affect battery performance, life, and safety. ICP-AES is generally used for the analysis of trace components, but the challenge is that certain elements, such as fluorine and silicon, are difficult to measure. Standardless FP method can improve the detection limit by adding fixed angle measurement that extends the integration time for the element of interest.



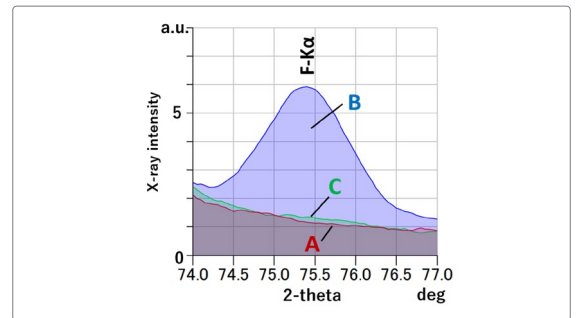


Figure 1: XRF qualitative chart of each sample

Figure 2: F-Kα qualitative chart of each

(ppm)

Sample	F	Na	Mg	Al	Si	S	Ca	Ti	Cr	Mn	Со	Ni	Cu	Zn	Zr	Pb
А	ND	ND	ND	22	100	57	ND	ND	ND	ND	ND	ND	ND	ND	ND	ND
В	9000	45	ND	2760	86	81	32	1590	44	120	41	210	ND	ND	16	ND
С	ND	690	ND	41	78	98	55	ND	ND	520	ND	29	22	ND	ND	ND

**Table 1:** SQX analysis results and theoretical standard deviations of each sample ND: less than LLD (detection limit value), LLD: 3 times statistical error in background intensity

**Conclusion:** For the analysis of trace component, fixed angle measurement can be applied to meet the required quantitation limit. From Fig.1 and Table 1, battery grade cathode materials (samples B and C) were found to contain impurity on the order of tens to thousands of ppm compared to LiFePO₄ reagent (sample A). This implies that the difference between the material grades is high. Furthermore, fluorine, which is difficult for ICP-AES, can be quantitatively analyzed simultaneously with other elements, as shown in Fig. 2.



**Equipment Used:** ZSX Primus IV





# Evaluation of Nanoscale Structural Changes in Primary Particles of Ncm by Electron Diffraction

Analysis: Cathode material

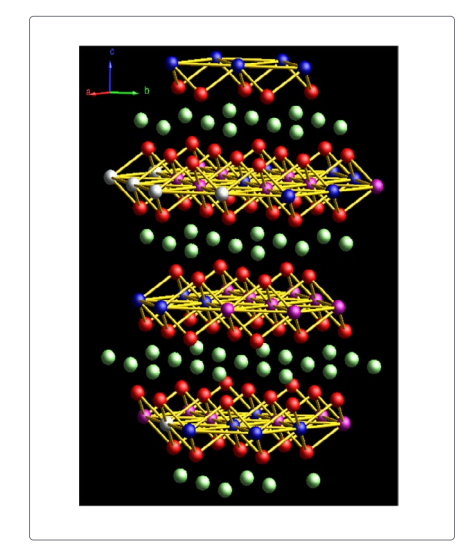
Use: Optimizing electrochemical performance

Analyzed materials:

LiNi<sub>x</sub>Co<sub>y</sub>Mn<sub>z</sub>O<sub>2</sub>, NCM

Crystal phase analysis

While NCM cathode materials contribute to high capacity, repeated cycles can cause strain and lattice disorder to accumulate inside the particles, leading to rapid performance degradation. Although it was previously difficult to directly observe the causes of such changes at the nanoscale, fully evaluating the three-dimensional extent of each Bragg reflection in electron-beam diffraction now makes it possible to treat each sub-micron-sized NMC particle as a single crystal and obtain highly accurate structural information. This enables the acquisition of high-precision structural information. Furthermore, it is possible to quantitatively understand where and how the strains, defects, and lattice distortions that occur in NCM cathode particles after charging and discharging change on a nanoscale.



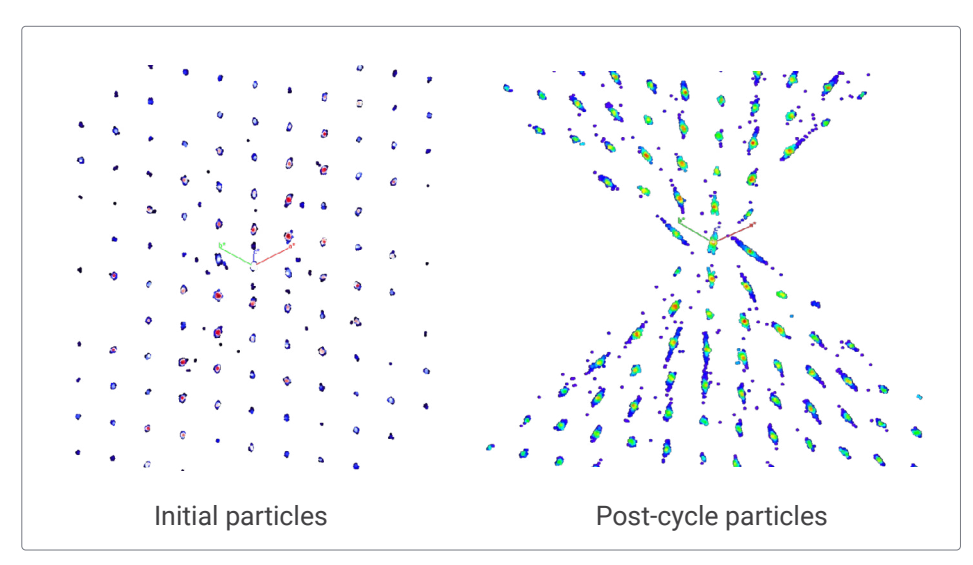


Figure 1: Crystal structure of NCM

Figure 2: Diffraction peaks of reciprocal lattice

**Conclusion:** Three-dimensional structural analysis of individual NCM primary particles by electron diffraction revealed clear structural changes after charge-discharge cycles. Initially, the diffraction peaks in reciprocal lattice space were mainly circular, but after charge-discharge cycling, the peaks were elongated, suggesting increased lattice distortion and structural disorder.







### Local Structure Analysis of Cathode Materials by PDF and RMC

**Analysis:** Cathode material

**Use:** Optimizing electrochemical performance

**Analyzed materials:** 

LiCoO<sub>2</sub>, LCO

⊕ Crystal phase analysis

Excess lithium cathodes are attracting attention as a key to high capacity, but structural disorder and performance instability caused by excess lithium have been a challenge. In contrast to the local structural disorder that tends to be overlooked in conventional structural analysis, X-ray total scattering and PDF (Pair Distribution Function) analysis can quantify where excess lithium atoms move, how the surroundings are distorted, and how the distortion changes during charging and discharging by refining local pair correlation in addition to the average lattice parameters. and how that distortion changes during charging and discharging can be quantitatively understood. This deep real-space insight is essential to understanding and ultimately controlling the effects of excess lithiation on cathode stability and performance.

Analysis Method Li - Li (Å)		Li σ (Å)	Disorder rate m
RMC	2.82	0.11	0.017

Table 1: Interatomic distances by structural analysis type

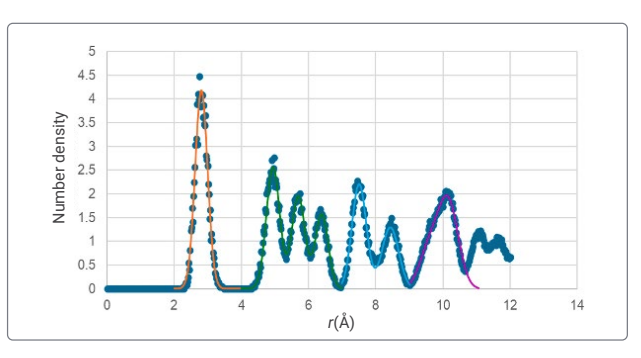
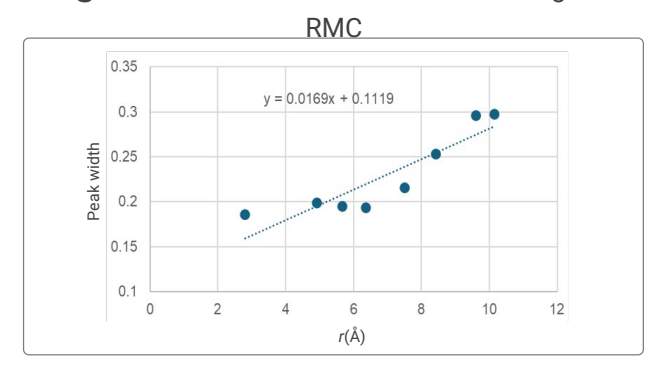


Figure 1: Li-Li distance calculated from big box



**Figure 2:** Peak width of Li-Li distance vs. each Li-Li distance σ

**Conclusion:** RMC analysis was performed on the PDF pattern of  $LiCoO_2$  (LCO) to analyze the peak width ( $\sigma$ ) corresponding to the Li-Li interatomic distance for each interatomic distance. As a result, it was confirmed that  $\sigma$  tends to increase as the interatomic distance increases. In general, the smaller  $\sigma$  is, the more stable and ordered the crystal structure is, and the larger  $\sigma$  is, the more disordered the structure is. Based on this relationship, the linear equation y (interatomic distance) = mx ( $\sigma$ ) + c (zero-point vibration  $\approx$  temperature factor) can be derived, and the disorder rate can be quantitatively evaluated from the slope m. Note that conventional single crystal structure analysis is limited to information on the average structure, but the RMC method can be used to extract such local structural changes. The quantitative information on the Li-Li distance obtained in this way may be used as an indicator to estimate the state of charge (SOC) of cathode materials and the amount of isolated particles that do not participate in charge-discharge cycles.



**Equipment Used:** SmartLab

Analysis Software: Smartlab Studio II





### Crystallite Size Analysis of Sodium-ion Battery Materials

**Analysis:** Sodium cathode material

**Use:** Optimizing electrochemical performance

**Analyzed materials:** 

NaFeO<sub>2</sub>

**Trystal phase analysis** 

Sodium-ion batteries have the advantage of abundant raw materials and low environmental impact, but there are challenges in securing high discharge voltage and capacity. It is known that the higher the crystallinity of  $\alpha$ -NaFeO<sub>2</sub>, which is expected to be used as a cathode material, the better the charge-discharge characteristics. Crystallinity evaluation by XRD is done by calculating crystallite size from peak widths and is useful for evaluating synthetic samples.

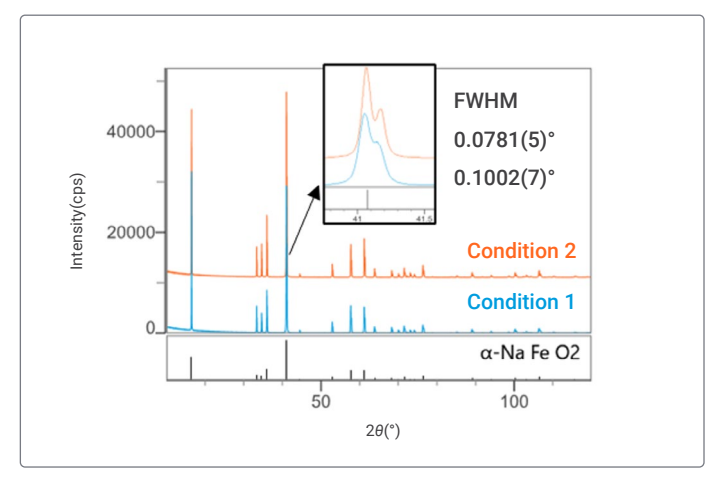


**Figure 1:** XRD patterns of α-NaFeO $_2$  synthesized under different conditions. Condition 1: 150°C, 48 hours; Condition 2: 220°C, 20 hours. Vertical axis is offset notation.

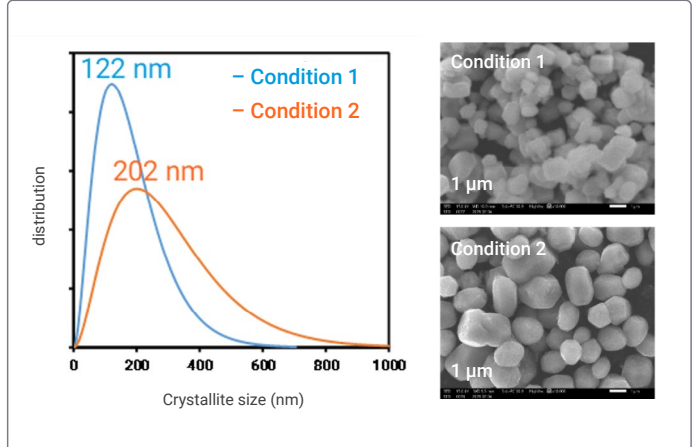


**Figure 2:** Crystallite size distribution analysis (left) and SEM images (right) of α-NaFeO<sub>2</sub> synthesized under different conditions.

**Conclusion:** Samples were prepared by hydrothermal synthesis. XRD patterns of two samples obtained under different conditions were compared. It was found that the peak width of the sample under condition 2 was smaller and the crystallite size was larger. In addition, the SEM images also showed that the grain size of the sample under condition 2 was larger, which was consistent with the results of the crystallite size analysis by XRD.



**Equipment Used:**SmartLab, SmartLab SE

Onboard Detector: XSPA-400 ER





### Compositional Analysis of Cathode Materials for Sodium Ion Batteries

Analysis: Sodium cathode material Analyzed materials:

**Use:** Optimizing electrochemical performance NaFeO,

**\*** Elemental Analysis

Sodium ion batteries are being developed as a next-generation battery to replace lithium ion batteries due to the abundance of resources and safety considerations. In particular, NaFeO<sub>2</sub> is expected to be a promising cathode material due to the abundance of its raw materials, Na and Fe. Compositional analysis is an important process in R&D and process control, and X-ray fluorescence analysis using the standardless FP method enables quick and easy evaluation of sample composition and impurities with simple pretreatment.

	Main component (mass%)		Impurities (ppm)						
	Na O <sub>2</sub>	Fe <sub>2</sub> O <sub>3</sub>	Al	Si	р	S	Cr	Mn	Cu
XRF analysis value	27.9	72.0	32	73	5	208	154	198	53

Table 1: Analysis Results

	Main component (molar ratio)		
	Na	Fe	
Expected value	1.00	1.00	
XRF analysis value	1.03	1.00	



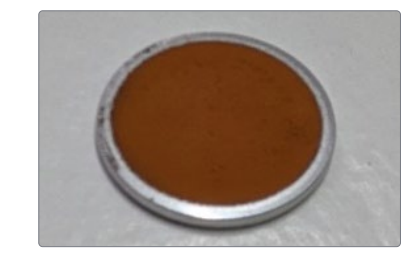


**Figure 1:** Pressure molding method sample preparation

**Conclusion:** Powder samples were pressed into pellet and subjected to X-ray fluorescence analysis using the standardless FP method. In the quantitative results obtained, the elemental ratios of Na and Fe were in good agreement with expected values. In addition, trace impurities in the range of a few ppm to 100 ppm such as Al, Si, and Cr were also detected, demonstrating the high sensitivity of this method and the effectiveness of simultaneous multi-element analysis. Using the standardless FP method, elemental compositions can be quickly and easily determined without standard samples.



**Equipment Used:** ZSX Primus IV





### **Operand Measurement Using a Coin Cell**

Analysis: Whole battery

**Use:** Improving battery performance

Phase transition analysis

**Analyzed materials:** 

Coin cell (Cathode NCM, anode Li, separator, electrolyte solution)

Operando measurements of lithium-ion batteries are generally performed on large X-ray diffractometers due to limitations in attachment size and the optics used. By preparing coin cell samples with an X-ray window, operando measurements can be performed on a variety of instruments.

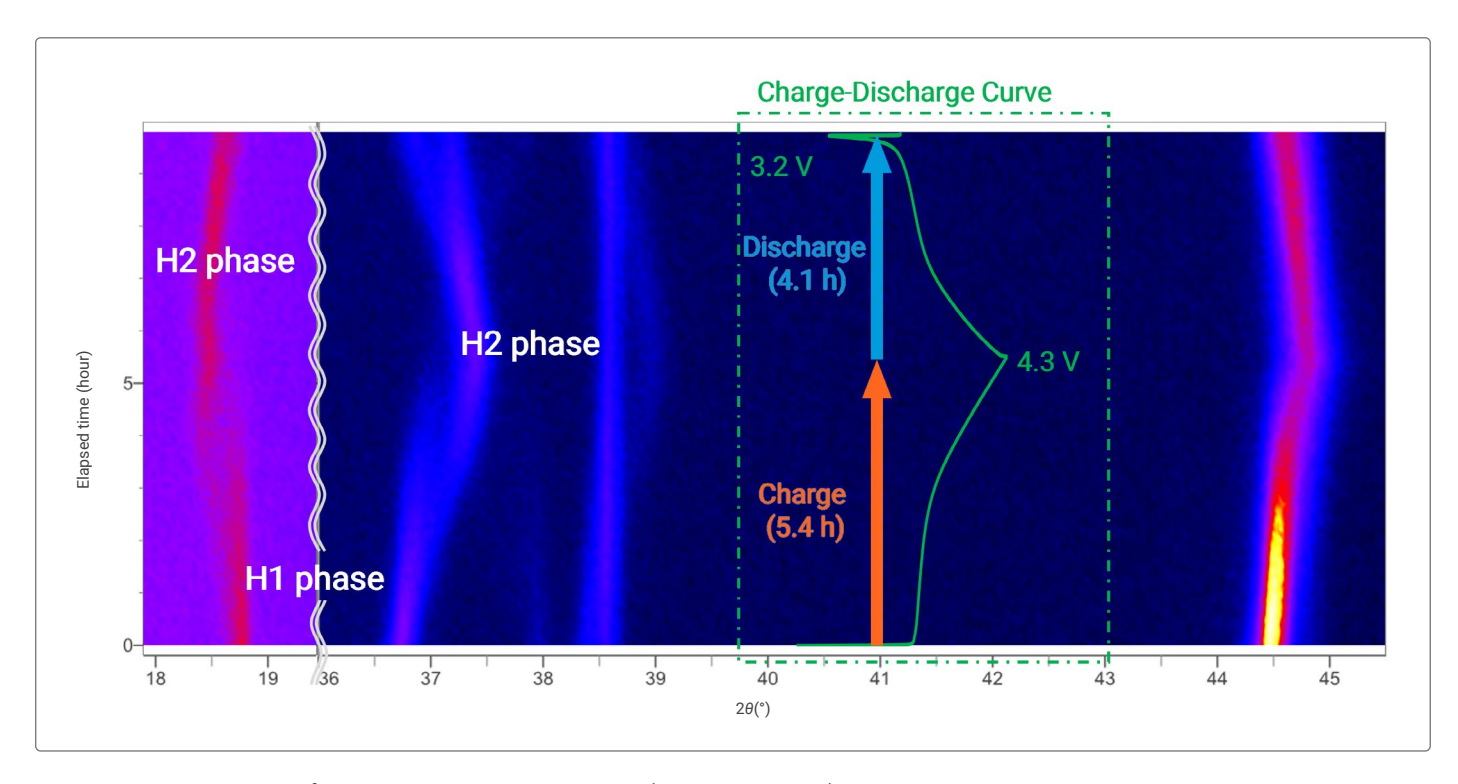


**Figure 1:** Elapsed time vs  $2\theta$  (color: intensity) and charge-discharge curve

**Conclusion:** The operando measurement clearly observed the crystallographic changes in the cathode material due to charging and discharging. The discontinuous and continuous changes in peak positions are attributed to the phase transition from H1 to H2 phase of NCM and the change in lattice constant.







# XRF Analysis Method for LPSCL Solid Electrolytes Under Non-Exposure to Air

**Analysis:** Sulfide solid electrolytes **Use:** Improving ionic conductivity

Analyzed materials:

**LPSC** 

**B** Elemental Analysis

In the development of all solid-state batteries, accurate composition evaluation of solid electrolytes is an important process that directly affects battery performance and safety. Sulfide-based solid electrolytes, in particular, have high ion conductivity, but they react with moisture in the air to produce toxic gases, so strict handling of the samples is required. Conventional ICP analysis involves complicated pretreatment such as acid decomposition of the sample and risks of exposure to the atmosphere, which poses problems in terms of worker safety and reproducibility of analysis. Against this background, there is a need for a "simpler, safer, non-atmospheric exposure" and "highly accurate compositional evaluation" method. In this method, powder samples are sealed in a double-sealed cell to ensure airtightness, enabling rapid XRF measurement of sulfide-based solid electrolytes in a non-destructive and non-air-exposed manner. This allows simplification of pretreatment and improvement of work efficiency while ensuring safety at the same time.

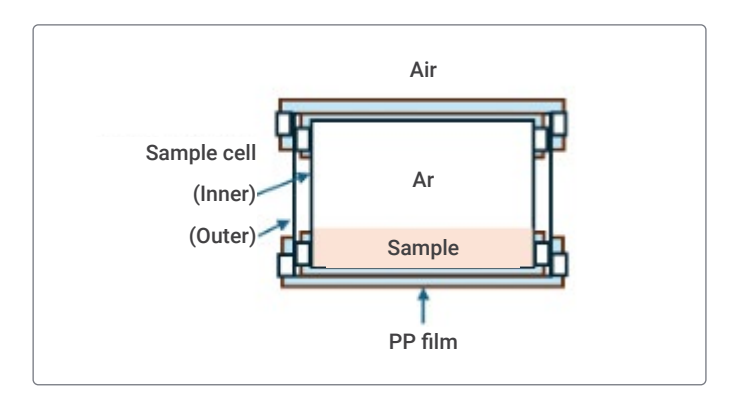


Figure 1: Schematic of double container

(Units mass %)

Component	Li	р	S	CI
Chemical composition	16	12	60	13
Analysis value	-	13.0	58.8	12.7

Table 1: Measurement results

**Conclusion:** In this study, LPSCI powder was sealed in a double container in a glove box and measured by XRF without exposure to air. The results for the main components were in good agreement with expected values, demonstrating the effectiveness of this non-destructive, rapid, and simple compositional analysis method. This approach will greatly streamline the quality control of solid electrolytes and the evaluation process in research and development, while ensuring safety.



**Equipment Used:** Supermini200

**Analysis Method:** Standardless FP method





### All-Solid-State Batteries Internal Structure Evaluation of Solid Electrolyte

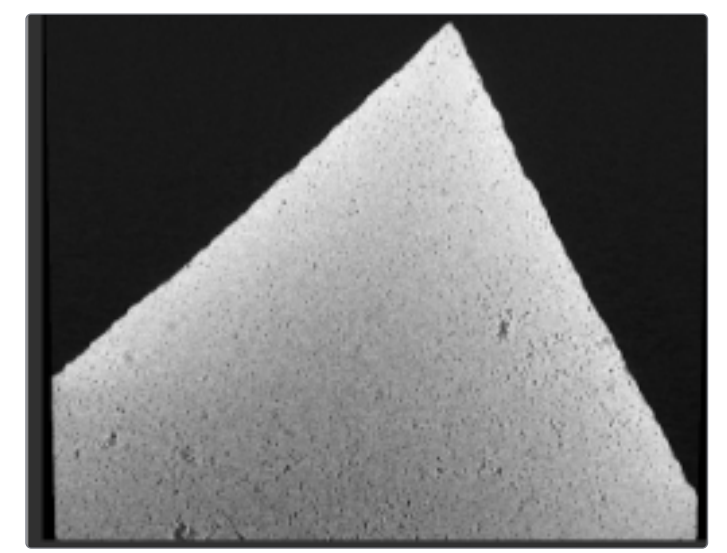
Analysis: All solid-state battery

**Use:** Optimizing electrochemical performance

Non-destructive analysis

Analyzed materials: All solid-state battery Oxide electrolytes

Improvement of ionic conductivity of solid electrolytes is essential to improve the performance of all solid-state batteries, and high-resolution observation of the internal structure is important to evaluate the performance. When using an electron microscope to observe a sample at high resolution, it is necessary to coat the sample surface with a conductive material for antistatic treatment, and in the case of untreated samples, accurate observation is not possible due to the effect of charging. By using nano3DX, which enables nondestructive 3D high-resolution observation of the inside of a sample, it is possible to evaluate the void space inside a solid electrolyte without antistatic treatment, which is expected to simplify battery design and improvement.



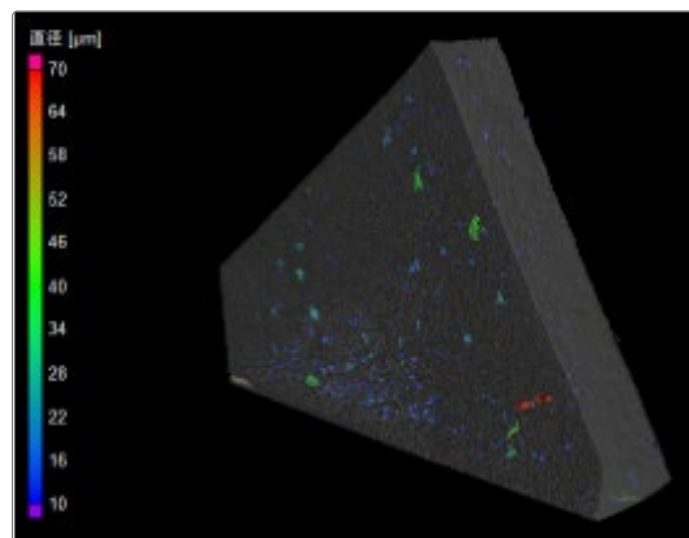


Figure 1: Tomogram

Figure 2: Pore analysis

**Conclusion:** A piece of a solid electrolyte was imaged with high-resolution by using 3D X-ray microscope, nano3DX, and multiple voids were observed inside the sample. Pores larger than 10  $\mu$ m inside the sample were evaluated, and the porosity was found to be 0.06%. Pores in a solid electrolyte may affect the ionic conductivity inside as well as the adhesion state with the cathode and anode on the surface. By evaluating the pore size of solid electrolytes, we can study the conditions for solid electrolyte preparation to improve performance.



**Equipment used:** nano3DX

**Analysis Software:** VGSTUDIO MAX





# Evaluation of Crystallite Size and Grain Size Distribution of Fuel Cell Materials by In-Situ XRD And SAXS

Analysis: Fuel cell
Use: Optimizing electrochem

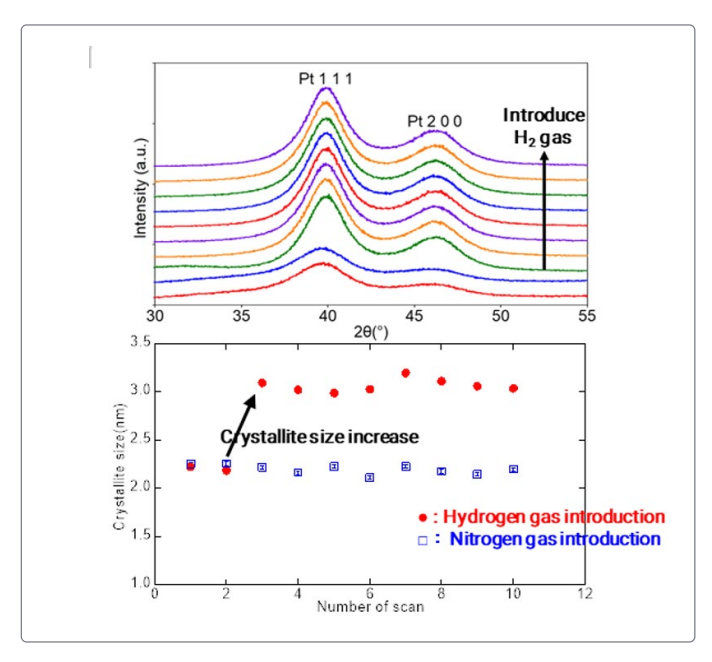
Optimizing electrochemical performance

Analyzed materials:

Pt as catalyst

Particle size and structure analysis

In fuel cells, it is known that the average particle size of the Pt catalyst used in the fuel electrode, which is a component material, affects the battery life. Such particle size variation can be evaluated using XRD and SAXS. In this study, the crystallite size of Pt nanoparticles was evaluated by in-situ XRD measurements in a hydrogen gas atmosphere (room temperature) using a corrosion-resistant infrared heated sample high temperature attachment. Small-angle X-ray scattering (SAXS) measurements were also performed before and after the introduction of hydrogen gas to investigate the average particle size and size distribution of Pt nanoparticles.



Before introduction of hydrogen gas
After introduction of hydrogen gas

**Figure 1:** XRD pattern with hydrogen gas introduction and crystallite size change of Pt nanoparticles

**Figure 2:** SAXS patterns before and after introduction of hydrogen gas and particle size distribution analysis of Pt nanoparticles

**Conclusion:** The introduction of hydrogen gas resulted in a sharp change in the diffraction peak shape of the XRD pattern, confirming an increase in the crystallite size of the Pt nanoparticles. The change in the slope of the SAXS profile also suggested a change in particle size. Thus, the ability to evaluate crystallite size and grain size under different environments is a useful method for elucidating the mechanism of structural changes in materials.



#### **Equipment Used:**

SmartLab SE, SmartLab, Reactor-X

### **Analysis Software:**

Smartlab Studio II

#### **Analysis Method:**

Crystallite size analysis, grain size analysis





# SAXS-RMC Method for Estimating 3D Structure of Pt/GDC Supported Nanoparticles

Analysis: Fuel cell

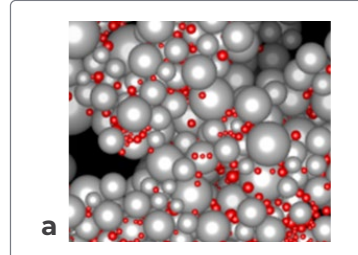
Use:

Optimizing electrochemical performance

**Analyzed materials:** Pt as catalyst

Particle size and structure analysis

Catalysts consisting of platinum nanoparticles supported on gadolinium-doped porous ceria (Gd-doped ceria: GDC) (Pt/GDC catalysts) have been reported to exhibit better four-electron oxygen reduction reaction activity than commercially available Pt/C catalysts¹. It is important to ensure that the reactions at the catalyst surface in the catalyst bed are facilitated, e.g., by the oxygen and hydrogen gas supply pathways. To understand these properties, it is useful to evaluate the three-dimensional structure of the entire catalyst layer, which is a complex aggregation of nanoparticles. However, with conventional observation methods, it is difficult to nondestructively determine how the nanoparticles are aggregated in three dimensions. By combining small-angle X-ray scattering (SAXS) and reverse Monte Carlo (RMC) methods, it is possible to estimate the three-dimensional aggregation structure of nanoparticles non-destructively and statistically.



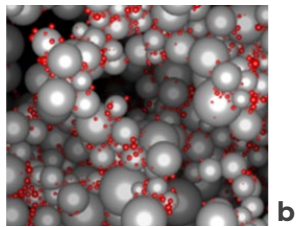
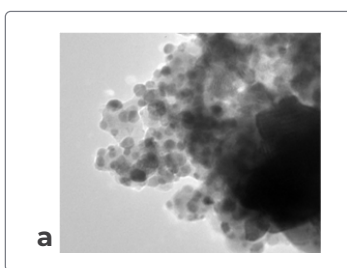
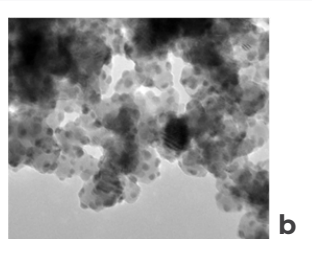


Figure 1: The resultant structural models obtained by RMC to match the observed SAXS patterns. Red and gray spheres for Pt and GDC particles, respectively.

a) Pt 50wt%, b) Pt 20wt%

Conclusion: The structural model constructed by the combination of SAXS and RMC methods was in good agreement with the TEM observation results. Furthermore, the pore size distribution calculated based on the model was in good agreement with the experimental results obtained by nitrogen gas adsorption, confirming the reproducibility of macroscopic structural indices. These results indicate that the SAXS-RMC method is a very useful 3D structural analysis technique that is superior in both visualization of local structure and statistical structure reproduction.





**Figure 2:** A typical TEM image. a) Pt 50wt%, b) Pt 20wt%

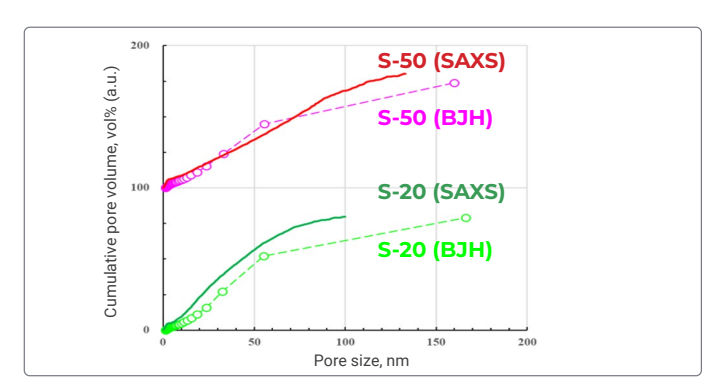


**Figure 3:** The BJH analysis result curves are shown in the dashed lines with the measurement data points in open circles. average curves of three RMC simulations run for SAXS patterns are shown in the solid lines.

<sup>1</sup>G. Shi, T. Tano, D. A. Tryk, A. liyama, M. Uchida, Y. Kuwauchi, A. Masuda and K. Kakinuma, *J. Catal*, **59-11**(2022), 582(7pp). Original paper: T. Iwata, K. Omote, K. Kakinuma, *Rigaku Journal*, **40** (2024), 1(pp11). K. Omote, T. Iwata, K. Kakinuma: Adv. *Theory Simul*. **7** (2023), 2300713(pp9).

### **Equipment Used:**

Small angle X-ray scattering system

## **Analysis Software:** SAXS3DM





### In-plane Adhesion Analysis of Fuel Cell (PEFC) Electrodes

Analysis: Fuel cell Analyzed materials: Use: Quality assurance Pt as catalyst

**\*** Elemental Analysis

In polymer electrolyte fuel cells (PEFCs), platinum (Pt) supported on carbon is used as an electrocatalyst, and it has been pointed out that the in-plane distribution of Pt may be involved in reaction bias and degradation. It is therefore important to evaluate not only the amount of Pt deposited, but also its distribution. We evaluated the in-plane deposition of Pt on PEFC electrodes using X-ray fluorescence analysis, which enables nondestructive analysis of composition and deposition amount.

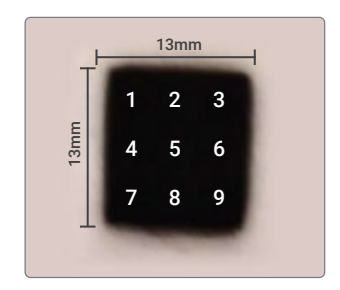


Figure 1: Sample and measurement coordinates

(1)	(2)	(3)		
0.191	0.184	0.171		
(4)	(5)	(6)	Max. 0.20	
0.171	0.167	0.163		
(7)	(8)	(9)	Min. 0.10	
0.163	0.142	0.139		
( ): Coordinate number				

**Table 1:** Analysis results for each coordinate [mg/cm<sup>2</sup>]

Number of measurements	Analytical value [mg/cm²]
1	0.168
2	0.168
3	0.167
4	0.167
5	0.167
6	0.167
7	0.168
8	0.166
9	0.166
10	0.166
mean value	0.167
greatest value	0.168
minimum value	0.166
range	0.002
standard deviation	0.001
Coefficient of variation (%)	0.5

**Table 2:** Results of simple 10 repetition measurement (Coordinates 5)

**Conclusion:** Point measurements were performed on a 13 mm square sheet coated with a Pt-supported carbon electrode for the 9 coordinates shown in Figure 1 under the conditions of 3 mm diameter and 60 seconds measurement time. Based on the obtained Pt La fluorescence intensity, the amount of Pt deposition was quantitatively evaluated by the standardless FP method. The analysis results shown in Table 1 confirm that the amount of Pt deposition tends to be higher in the upper left of the diagonal direction, indicating that there is a variation in the in-plane distribution. As shown in Table 2, the measurement was repeated 10 times under the same conditions at the position of coordinate 5, and the coefficient of variation was 0.4%, indicating extremely good reproducibility.



**Equipment Used:** NEX DE

**Analysis Method:**Standardless FP method





[mg/cm<sup>2</sup>]

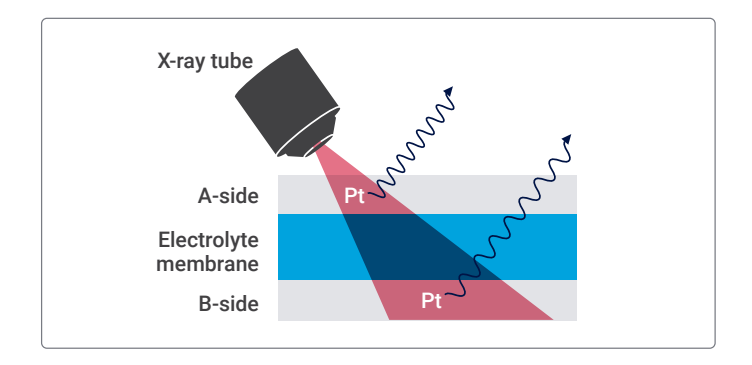
# Analysis of Adhesion within Both Sides of a Fuel Cell (PEFC) Electrode

**Analysis:** Fuel cell **Use:** Quality assurance

Analyzed materials: Pt as catalyst

Elemental Analysis

In a polymer electrolyte fuel cell (PEFC: Polymer Electrolyte Fuel Cell), a cathode layer and an anode layer are placed on both sides of the electrolyte membrane. Since the amount of platinum (Pt) catalyst on each electrode layer is different, each layer must be managed separately. Conventional control methods require each surface to be measured separately, resulting in a large workload and time cost. X-ray fluorescence analysis is an effective method for efficiently solving these problems because it has high penetrating power, is nondestructive, and can simultaneously evaluate the amount of Pt adhered on both surfaces in a single measurement.



 Measurement surface
 A-side
 B-side

 Analysis value
 0.201
 0.42

 Design value
 0.203
 0.405

 Relative error (%)
 1.0
 3.7

Figure 1: Schematic diagram of measurement

**Table 1:** Analysis results for each aspect

**Conclusion:** Both sides (A-side and B-side) of the electrolyte membrane sheet coated with platinum-loaded carbon electrode were measured for 60 seconds using X-ray fluorescence of platinum and quantitatively analyzed by the thin-film FP method. As shown in Table 1, the analysis results for each measurement point agreed with the design values for each surface within ±5% relative error, confirming that the platinum loading in this film formation process was properly controlled.



**Equipment Used:** NEX DE

Analysis Method: Standardless FP method





# Evaluation of Water Absorption and Swelling in Polymer Electrolyte Membranes

Analysis: Fuel cell Analyzed materials: Use: Evaluation of thermal stability Electrolyte membrane

**In Tale 1** Thermal Analysis

In the fuel cell operating environment, changes in temperature and humidity affect the expansion and contraction of materials. Dimensional changes due to water absorption in polymer electrolyte membranes can have a significant impact on cell sealing and adhesive durability. There are limited methods to evaluate these properties in a humid environment, and STA and TMA with controlled humidity are effective approaches in material design and selection.

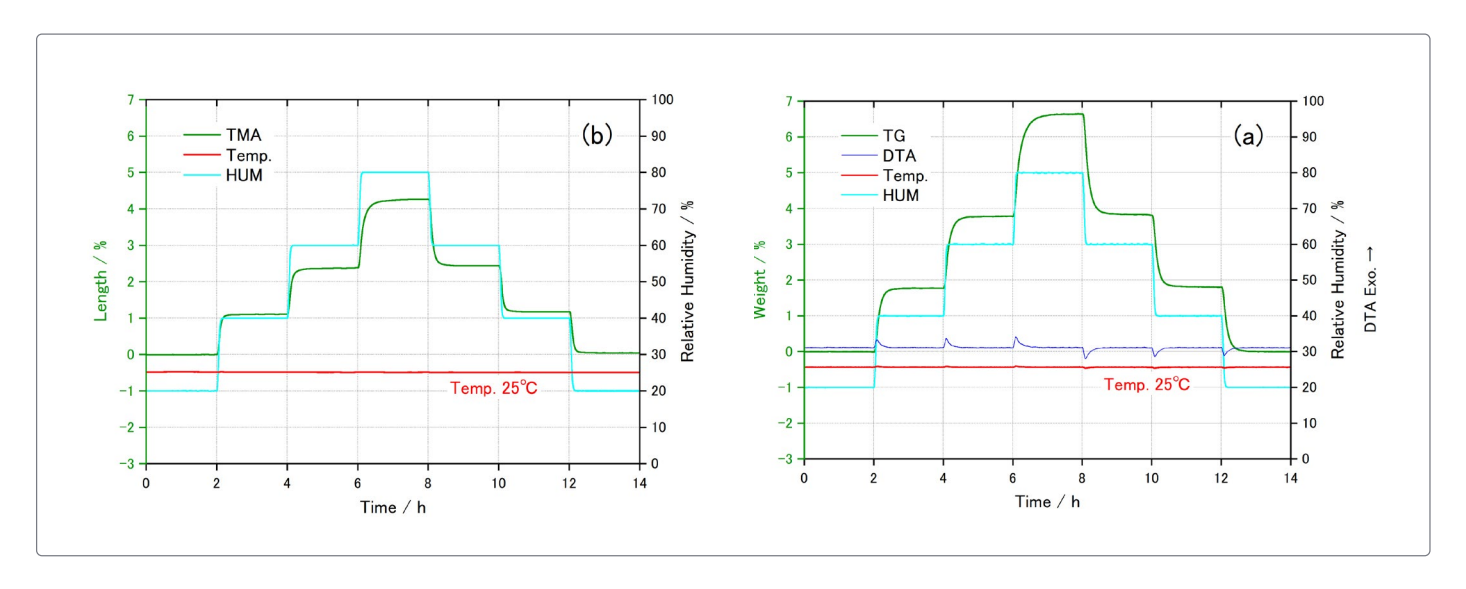


**Figure 1:** (a) weight change and (b) dimensional change of polymer electrolyte membranes as a function of relative humidity.

**Conclusion:** STA measurements under humidity-controlled conditions allow quantitative evaluation of water absorption by measuring the weight change of a sample under each relative humidity condition. TMA can also be used to determine the swelling behavior under each humidity condition.









# Internal Structure Evaluation of Fuel Cell Membrane Electrode Assembly (MEA)

**Analysis:** Fuel cell **Use:** Optimizing electrochemical performance

Analyzed materials:

MEA, Membrane Electrode Assembly

Non-destructive analysis

For improving the performance and quality of fuel cells, it is important to evaluate the internal structure of the gas diffusion layer (GDL) in the membrane electrode assembly (MEA), a multifunctional base material responsible for gas diffusion, electron collection, and discharge of produced water. GDLs are composed of low-density materials such as carbon fiber, and conventional X-ray CT imaging using high-energy X-rays does not provide contrast because X-rays are not absorbed by GDLs, making it difficult to analyze pore size and diffusion pathways. The nano3DX, which is capable of low-energy X-ray CT imaging, makes it possible to visualize and evaluate the structure of GDLs, and is expected.

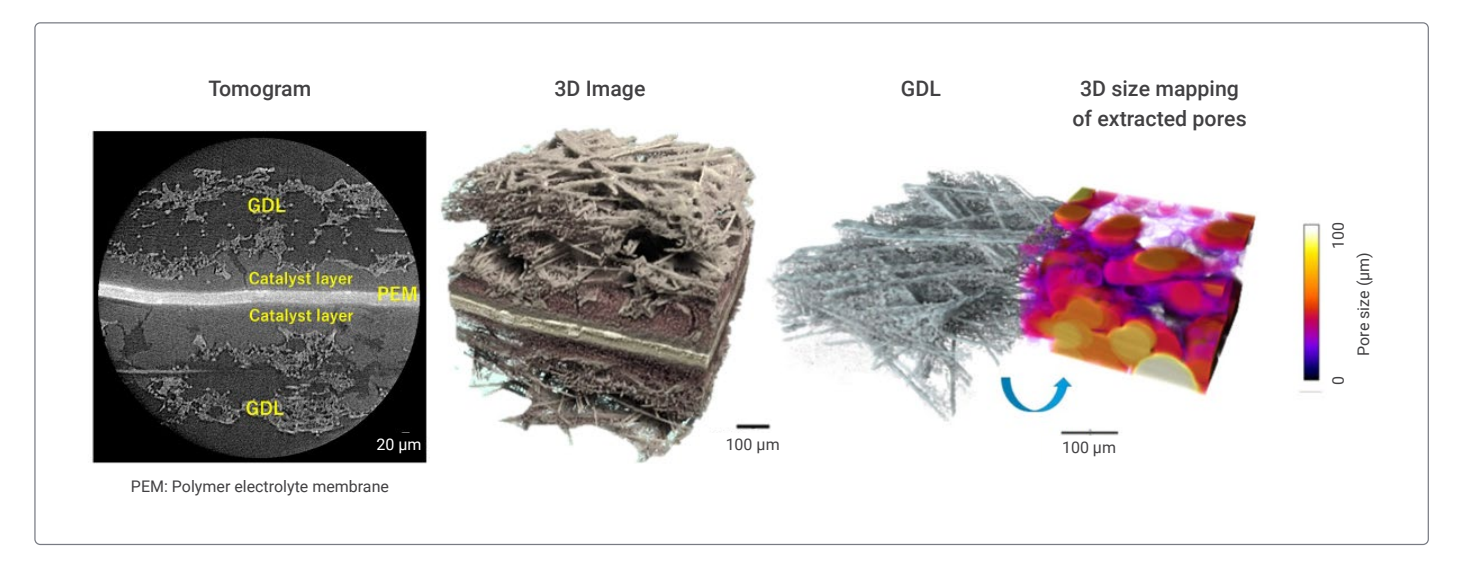


**Figure 1:** X-ray CT image of a membrane electrode assembly (MEA) and analysis of gas diffusion layer (GDL) pores.

**Conclusion:** CT imaging using low-energy characteristic X-rays of the Nano3DX enabled high-contrast and clear observation of GDLs even in the presence of electrolyte membranes with high-density platinum catalyst attached. By visualizing the internal structures of all the substrates comprising the prototype MEA in three dimensions and quantitatively evaluating structural indices such as the GDL pore size, it will be possible to study the optimization of the MEA preparation conditions.



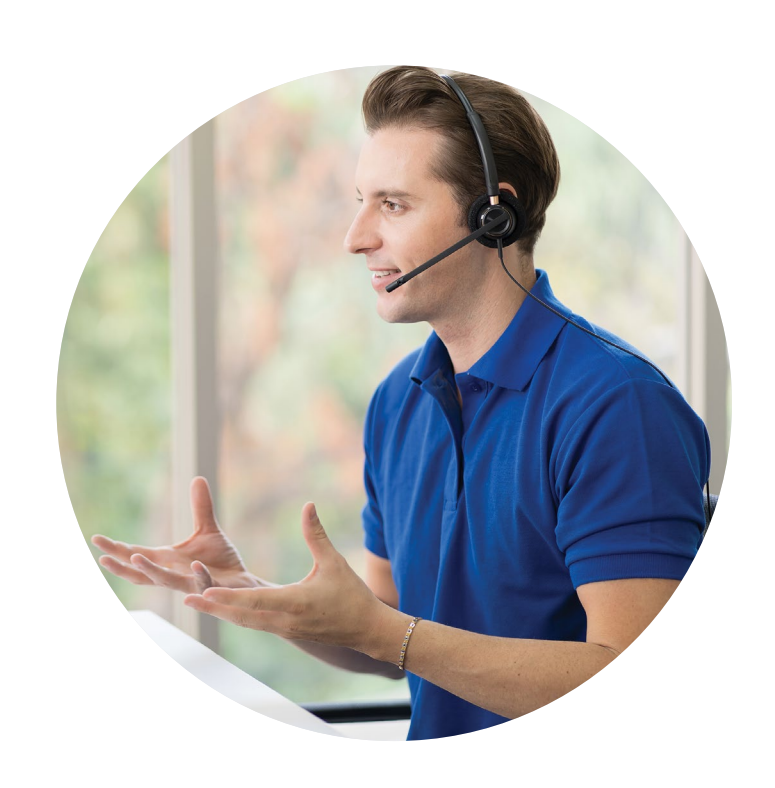


### **Contact Us**

Whether you have a question about battery analysis, want a demo, or are interested in using our instruments, we're here to help.



Contact Us Online: rigaku.com/talk-to-an-expert



### **Rigaku Locations**

#### **Rigaku Corporation (Tokyo)**

3-9-12, Matsubara-cho Akishima-shi, Tokyo 196-8666 Japan E-mail address info-gsm@rigaku.co.jp Phone number +81 42-545-8111

## Rigaku Beijing Corporation

2601A, Tengda Plaza, No. 168, Xizhimenwai Ave. Haidian District, Beijing 100044 China E-mail address info@rigaku.com.cn Phone number

#### **Rigaku Americas**

9009 New Trails Drive The Woodlands, TX 77381 United States E-mail address info@rigaku.com Phone number +1-281-362-2300

## Rigaku Asia Pacific PTE LTD

10 Anson Road, #22-04, International Plaza 079903 Singapore E-mail address rapp@rigaku.com Phone number

#### Rigaku Europe SE

Hugenottenallee 167 Neu-Isenburg 63263 Germany E-mail address rese@rigaku.com Phone number +49 6102 77999 51

